

# **RPSEA**

## ***Final Report***

***09123-18.FINAL***

Jyun-Syung Tsau, Mark Ballard, TORP, University of Kansas

### ***Characterization of Potential Sites for Near Miscible CO<sub>2</sub> Applications to Improve Oil Recovery in Arbuckle Reservoirs***

**09123-18**

**September 30, 2014**

Jyun-Syung Tsau  
Associate Scientist  
TORP, University of Kansas  
The University of Kansas Center for Research, Inc.  
2385 Irving Hill Road, Lawrence, KS 66045-7563

## LEGAL NOTICE

This report was prepared by the *University of Kansas Center for Research, Inc.* as an account of work sponsored by the Research Partnership to Secure Energy for America, RPSEA. Neither RPSEA, members of RPSEA, the National Energy Technology Laboratory, the U.S. Department of Energy, nor any person acting on behalf of any of the entities:

- a. **MAKES ANY WARRANTY OR REPRESENTATION, EXPRESS OR IMPLIED WITH RESPECT TO ACCURACY, COMPLETENESS, OR USEFULNESS OF THE INFORMATION CONTAINED IN THIS DOCUMENT, OR THAT THE USE OF ANY INFORMATION, APPARATUS, METHOD, OR PROCESS DISCLOSED IN THIS DOCUMENT MAY NOT INFRINGE PRIVATELY OWNED RIGHTS, OR**
  
- b. **ASSUMES ANY LIABILITY WITH RESPECT TO THE USE OF, OR FOR ANY AND ALL DAMAGES RESULTING FROM THE USE OF, ANY INFORMATION, APPARATUS, METHOD, OR PROCESS DISCLOSED IN THIS DOCUMENT.**

**THIS IS A FINAL REPORT. THE DATA, CALCULATIONS, INFORMATION, CONCLUSIONS, AND/OR RECOMMENDATIONS REPORTED HEREIN ARE THE PROPERTY OF THE U.S. DEPARTMENT OF ENERGY.**

**REFERENCE TO TRADE NAMES OR SPECIFIC COMMERCIAL PRODUCTS, COMMODITIES, OR SERVICES IN THIS REPORT DOES NOT REPRESENT OR CONSTITUTE AND ENDORSEMENT, RECOMMENDATION, OR FAVORING BY RPSEA OR ITS CONTRACTORS OF THE SPECIFIC COMMERCIAL PRODUCT, COMMODITY, OR SERVICE.**

## **ABSTRACT**

The study from a previous laboratory research project funded by RPSEA/NETL indicated that favorable mechanisms to improve oil recovery by injection of CO<sub>2</sub> at near miscible conditions are achievable at reservoir temperature at the Ogallah unit in Kansas. The initial plan of this study was to apply various engineering tests to characterize this mature oil field for a future pilot test of near miscible CO<sub>2</sub>. The plan was modified with the approval of RPSEA later to continue the project with objectives to 1) use an integrated methodology to construct an improved geological model in the Ogallah unit, 2) demonstrate the feasibility of CO<sub>2</sub> near miscible injection to mobilize the oil with a single well pilot test in an oil field produced from the Arbuckle formation, and 3) conduct reservoir simulation with the companion reservoir model to investigate the reservoir performance of near miscible CO<sub>2</sub> flooding applications.

The pilot test consists of a single well chemical tracer test before and after CO<sub>2</sub> injection on a selected well producing from the Arbuckle formation. The effectiveness of CO<sub>2</sub> displacement efficiency was determined by the reduction of oil saturation measured from the tracer tests. More than seven oil fields producing from Arbuckle reservoirs were considered in selection of a candidate well for the pilot test. The final pilot test was conducted at a well producing from the Arbuckle formation at reservoir temperature and pressure of 106 °F, 1150 psi respectively. The minimum miscibility pressure (MMP) determined was 1500 psi at reservoir temperature. The oil saturation measured from the two tracer tests were 0.23 and 0.20 respectively. A reduction of oil saturation by 0.03 represents a 13% improvement of oil displacement in tertiary oil recovery, which results from the displacement of CO<sub>2</sub> injection at near miscible conditions.

In the computational studies, the effect of CO<sub>2</sub> injection scheme and pattern on the oil recovery efficiency was examined. The average reservoir pressure was maintained at the near miscible condition during CO<sub>2</sub> injection as the pressure was supported by the underling aquifer. The displacement efficiency was found to vary slightly with different injection pattern and scheme. In general, the displacement efficiency in a 47 acre lease model is improved from 39 % to 46 % on average with continuous CO<sub>2</sub> injection and to 49% with WAG injection at near miscible conditions. The oil mobilized by CO<sub>2</sub> displacement at near miscible conditions is observed in the model at production wells in the target lease and surrounding leases.

**THIS PAGE INTENTIONALLY LEFT BLANK**

# TABLE OF CONTENTS

	<u>Page</u>
TABLE OF CONTENTS	i
LIST OF TABLES	ii
LIST OF FIGURES	iii
1. INTRODUCTION .....	1
2. COMPUTATIONAL STUDY .....	4
2.1 Background Information .....	4
2.2 Improved Geological Model .....	5
2.2.1 Arbuckle Carbonate Classification.....	7
2.2.2 Arbuckle Sandstone Classification.....	8
2.3 Reservoir Model .....	14
2.4 Production History.....	15
2.5 Primary Production Simulation .....	17
2.6 Simulation of Carbon Dioxide Injection .....	23
2.6.1 Continuous CO <sub>2</sub> Injection .....	27
2.6.2 Water Alternating Gas Injection .....	33
3. SINGLE WEL PILOT TEST .....	38
3.1 Candidate Well Selection .....	38
3.2 Field Operation .....	41
3.2.1 First Tracer Test .....	43
3.2.2 CO <sub>2</sub> Injection .....	43
3.2.3 Second Tracer Test .....	44
3.3 Computation Modeling .....	47
4. SUMMARY AND CONCLUSIONS .....	52
5. TECHNOLOGY TRANSFER .....	54
ACKNOWLEDGEMENT .....	56
REFERENCES .....	57

## LIST OF TABLES

		<u>Page</u>
Table 1	Cementation m and mean RFN values .....	8
Table 2	Cementation factor m and mean FZI .....	9
Table 3	PVT data used in black oil simulator .....	18
Table 4	Lumped compositional description of reservoir fluid .....	24
Table 5	Summary of production and injection results of case A .....	29
Table 6	Summary of injection and production results on lease 3 with different injection pattern .....	33
Table 7	Summary of WAG process on lease 3 with different injection pattern ....	36
Table 8	Oil fields considered for single well pilot test .....	38
Table 9	Candidate well list .....	39
Table 10	Partition coefficient K value measurement .....	42
Table 11	Design of first chemical tracer test .....	43
Table 12	Design of second chemical tracer test .....	45
Table 13	Residual oil saturation calculated from the simulation .....	50
Table 14	Effect of CO <sub>2</sub> injected volume on displacement efficiency at near miscible conditions .....	50

## LIST OF FIGURES

		<u>Page</u>
Figure 1	Schematic representation of CO <sub>2</sub> oil recovery efficiency as a function of pressure .....	1
Figure 2	Crossplot of permeability vs. porosity of the Arbuckle dolomite core samples from Ogallah unit .....	7
Figure 3	Relationship between m and Log RFN of the Arbuckle dolomite samples from Ogallah unit .....	8
Figure 4	Crossplot of porosity and permeability of sandstone core samples from Ogallah unit .....	9
Figure 5	Relationship between m and FZI of Arbuckle sandstone .....	10
Figure 6	The lithofacies defined by the core corresponding electrofacies identified from the well logs in carbonate .....	11
Figure 7	The lithofacies defined by the core, corresponding electrofacies identified from the well logs in sandstone .....	11
Figure 8	Comparison between porosity estimation based on constant m value and variable m values .....	12
Figure 9	The permeability prediction by using linear fit calculation and electrofacies with petrophysical classifier in sandstone .....	13
Figure 10	The permeability prediction by using linear fit calculation and electrofacies with petrophysical classifier (on the right) in carbonate .....	13
Figure 11	Porosity and permeability distribution of the Ogallah field .....	14
Figure 12	Structure top of Ogallah unit (subsea level).....	15
Figure 13	Example of cross-section view of Ogallah unit .....	15
Figure 14	Map of lease boundary and well location .....	16
Figure 15	Annual production history of Lease 3.....	17
Figure 16	Relative permeability curves of oil and water .....	18
Figure 17	Average reservoir pressure during primary production .....	20
Figure 18	Water oil ratio history match of well 1-6 and 6-1.....	20

	<u>Page</u>
Figure 19 Simulated movement of water-oil contact during primary production period from year 1952 to 2010.....	21
Figure 20 Lease production history match during primary production .....	22
Figure 21 Comparison of lease production history between models .....	23
Figure 22 Relative permeability of gas and oil used in gas injection process .....	24
Figure 23 Grid system of lease 3.....	25
Figure 24 Pattern design in CO <sub>2</sub> injection on lease 3.....	26
Figure 25 Permeability and porosity map of layer 10.....	26
Figure 26 Comparison of recovery factor and average reservoir pressure in case A .....	27
Figure 27 Production history of well 1-7, which is located 930 feet northwest of CO <sub>2</sub> injector 3-4.....	28
Figure 28 CO <sub>2</sub> and oil saturation distribution for injection pattern A.....	29
Figure 29 Production performance at producer 3-2 during simulated CO <sub>2</sub> injection .....	30
Figure 30 CO <sub>2</sub> and oil saturation distribution for injection pattern B .....	30
Figure 31 CO <sub>2</sub> and oil saturation distribution for injection pattern C .....	31
Figure 32 CO <sub>2</sub> and oil saturation distribution for injection pattern D .....	31
Figure 33 CO <sub>2</sub> and oil saturation distribution for injection pattern E .....	31
Figure 34 CO <sub>2</sub> and oil saturation distribution for injection pattern F .....	32
Figure 35 Comparison of average reservoir pressure under different production conditions .....	34
Figure 36 Production performance of well 3-2 during WAG injection .....	35
Figure 37 Oil rate responding to different injection schemes at well 1-7.....	35
Figure 38 Locations of selected oil fields in Kansas .....	39
Figure 39 MMPs determined with a swelling/extraction test on sample oil from candidate well .....	40
Figure 40 Neutron density log with well configuration of candidate well for the pilot test .....	41
Figure 41 Schematic representation of typical tracer profiles during backflow for interpretation .....	42

	<u>Page</u>
Figure 42 CO <sub>2</sub> injection history with downhole pressure and temperature measurements .....	44
Figure 43 Produced tracer profiles from the first chemical tracer test .....	46
Figure 44 Production tracer profile from the second tracer test after CO <sub>2</sub> injection .....	47
Figure 45 Oil saturation distribution at the end of CO <sub>2</sub> injection .....	48
Figure 46 Oil saturation distribution at the end of water injection .....	48
Figure 47 Pressure distribution from the simulation calculation indicating the pressure inside the radius of investigation (20 ft) is maintained at near miscible condition with 2 PV CO <sub>2</sub> injection .....	49
Figure 48 Pressure distribution from the simulation calculation indicating the pressure inside the radius of investigation (20 ft) is maintained at near miscible condition with 4 PV CO <sub>2</sub> injection .....	49

## 1. INTRODUCTION

Miscibility of CO<sub>2</sub> in oil is a function of pressure and temperature (as well as the composition of the oil and other factors). In the reservoir temperature might be taken as a constant and we can view miscibility as a function of pressure only. With greater pressure comes greater miscibility and concomitant oil recovery from the porous media until pressures above the minimum miscibility pressure (MMP), above which little additional incremental oil is recovered.

In a relative way the relationship between pressure and oil recovery for CO<sub>2</sub> injection and oil recovery from a porous media has this form (Figure 1):

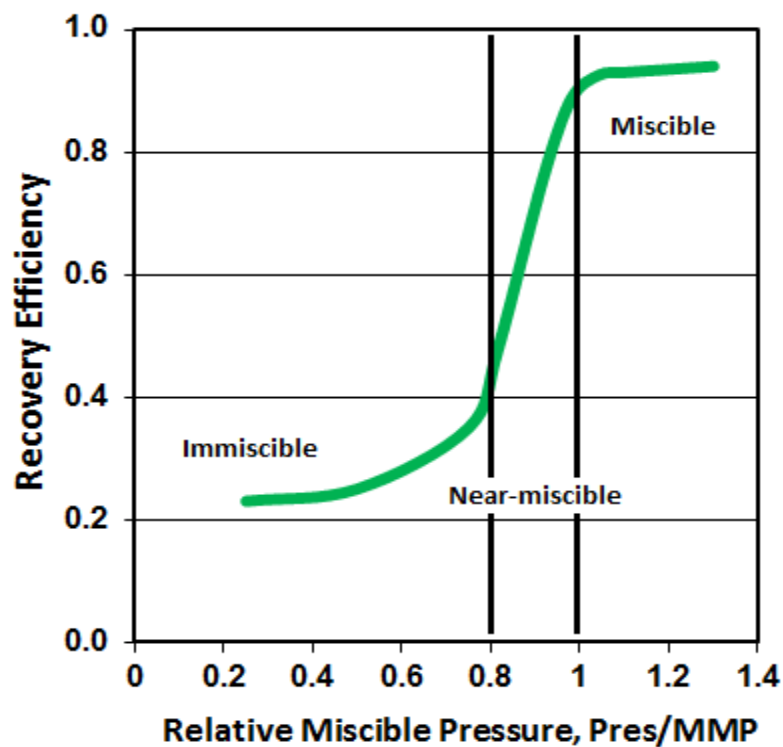


**Figure 1: Schematic representation of CO<sub>2</sub> oil recovery efficiency as a function of pressure.**

Carbon dioxide injection at miscible conditions to recover immobile oil has been practiced by industry for many years. The application of CO<sub>2</sub> injection to oil fields at shallower depths and lower pressures where CO<sub>2</sub> is at near miscible conditions is not broadly investigated. Significant oil resources in the United States could be recovered with additional understanding of near miscible approaches to oil recovery. The study from a previous laboratory research project funded by RPSEA/NETL indicated that favorable mechanisms to improve oil recovery by

injection of CO<sub>2</sub> at near miscible conditions, which is at a pressure of 200 psi below the Minimum Miscibility Pressure (MMP) at reservoir temperature in the Arbuckle reservoir at the Ogallah field (Tsau, 2010)

The favorable mechanisms for oil recovery with near miscible CO<sub>2</sub> injection include swelling, reduction of oil viscosity, and extraction of light components. The favorable laboratory results prompted a follow up research proposal to characterize potential sites among Arbuckle reservoirs for future field application of near miscible CO<sub>2</sub> flooding.

This project describes a research program to evaluate the application of CO<sub>2</sub> displacement at near miscible pressures for improved oil recovery (IOR) for small producers. The initial proposal focused on characterization of the Ogallah oil field produced from the Arbuckle formation with individual well transient pressure tests, multiple well interference tests, single well tracer tests, and interwell tracer tests. All tests were designed to determine the nature of the flow paths and average properties in the reservoir, to assess the effect of geology on process performance, to calibrate a reservoir simulation model, and to identify operational issues and concerns for future IOR applications. This proposal was revised later, however, because of the withdrawal from the research partnership by the original operator. The revised proposal retains the main objective of the original proposal in characterization of potential sites for near-miscible CO<sub>2</sub> injection to improve oil recovery for small producers but moved the test field from the Ogallah field to another suitable oil field (Dreiling) with a new proposed design involving single well pilot tests.

The Ogallah field remains a target reservoir in the simulation study. By using vintage logs such as microresistivity logs commonly used in the early 50's with an integrated characterization method, the geological model is more representative of the oil field and therefore the companion reservoir model was used in a reservoir simulation study on the CO<sub>2</sub> injection process. An individual well in another oil field, the Dreiling field (also produced from the Arbuckle formation) was used for the field portion to experimentally demonstrate the effectiveness of CO<sub>2</sub> application at near miscible conditions.

The pilot design consists of a single well chemical tracer test before and after CO<sub>2</sub> injection. The first chemical tracer test was performed to determine the oil saturation in the formation prior to CO<sub>2</sub> injection. That was followed by injecting CO<sub>2</sub> at pressures below MMP with a follow up water displacement, then followed by a second tracer test performed to

determine the remaining oil saturation. The effectiveness of CO<sub>2</sub> displacement was determined by the reduction of oil saturation measured from the tracer tests.

More than seven oil fields producing from Arbuckle reservoirs were considered in selection of a candidate well for the pilot test. The pilot test was finally conducted on Dreiling #10 in the Dreiling field, Ellis County, Kansas. Downing-Nelson Oil Company is the operator of the oil field. The reservoir temperature was 106 °F and well shut in pressure was 1150 psi. The minimum miscibility pressure (MMP) determined was 1500 psi at reservoir temperature. The single well pilot test was applied without further changes to the design. The oil saturation measured from the two tracer tests was 0.23 and 0.20 respectively. A reduction of oil saturation by 0.03 represents a 13% improvement of oil displacement in tertiary oil recovery, which results from the displacement of CO<sub>2</sub> injection at near miscible conditions.

This report is divided into two major parts. The first part describes construction of a geological model with a methodology for characterization of a mature oil field, utilization of a reservoir model with a commercial simulator in reservoir simulation, and discusses the simulation results on improvement of oil recovery by CO<sub>2</sub> injection at near miscible conditions. The second part describes a pilot test conducted in a well producing from the Arbuckle formation to demonstrate the feasibility of using CO<sub>2</sub> injection at near miscible conditions to mobilize the oil.

Completion of this program provides the assessment of the effectiveness of CO<sub>2</sub> displacement at near-miscible pressures, which are below minimum miscibility pressure (MMP), and make it possible to determine the potential of CO<sub>2</sub> flooding in relatively shallow reservoirs. The Arbuckle is a huge oil resource in Kansas wherein the field operating pressure is generally below MMP. Attainment of the research objectives makes future field tests available for CO<sub>2</sub> near-miscible displacement.

## **2. COMPUTATIONAL STUDY**

The first part of this report describes construction of a geological model with a methodology for characterization of a mature oil field, utilization of a reservoir model with a commercial simulator in reservoir simulation, and discusses the simulation results on improvement of oil recovery by CO<sub>2</sub> injection at near miscible conditions.

It summarizes the methodologies applied to 1) develop a geological model and a reservoir model, 2) conduct a simulation study for history match of the primary production, and 3) investigate the effect of near miscible CO<sub>2</sub> injection on the oil recovery in the target oil reservoir. The target oil field, the Ogallah unit, is located in Trego County, Kansas. The unit produces from the Arbuckle formation (3950-4060 ft) and other formations above the Arbuckle (Marmaton and Lansing-Kansas City).

The geological model developed in this study was based on an integrated methodology combining cluster analysis with geostatistical methods to incorporate core and log data. The model-based clustering methods applied a transformation relationship between core and well logs and were developed to predict porosity, permeability and rock type in the model (Teh, et al., 2011, 2012). The phase behavior model developed from the phase behavior study (Tsau et al., 2010) was used with the geological model to form the reservoir model. A commercial simulator, IMEX (Computer Modeling Group, Inc.) was used to simulate the primary production history. A compositional simulator, GEM (CMG Inc.) was used to investigate the potential of using carbon dioxide at near miscible conditions for improvement of oil recovery.

### **2.1 Background Information**

Arbuckle reservoirs are a significant resource in Kansas for improved oil recovery. These reservoirs have produced an estimated 2.2 billion barrels of oil representing 35% of the 6.1 billion barrels of total Kansas oil production (Franseen et al., 2004). Most Arbuckle reservoirs have active water drives, which have maintained reservoir pressure at 1000-1100 psig for nearly 50 years even though millions of barrels of fluid have been produced. Of course, this works both ways. It is theorized that any attempt to raise the reservoir pressure in the Arbuckle would simply push back this aquifer influx and not achieve the desired pressure rise. Initial studies of CO<sub>2</sub> miscible flooding indicated that miscibility is not achievable at the reservoir

operating pressure in most Arbuckle reservoirs. For example, the Arbuckle reservoir oil in the Bemis-Shutts field has an MMP of 1400 psi while the current operating pressure is 1100 psi in a large portion of the field (Franseen et al., 2003). The Arbuckle reservoir in this study, the Ogallah unit, has an MMP of 1350 psi while the current reservoir operating pressure is in the neighborhood of 1150 psig. The core flow test in the laboratory study indicated that at least 50% of remaining oil could be recovered by CO<sub>2</sub> injection at current reservoir operating pressure (Bui et al., 2010).

The Ogallah field is located in Trego County, Northeastern Kansas along the west side of the Central Kansas uplift. The primary producing formation in this study is the Arbuckle at 3950-4000 ft. The formation is associated with structural highs on the Central Kansas uplift and is thin to absent in parts of Northeastern Kansas (Franseen, et al., 2004).

Because of a lack of modern porosity logs available from the field, the microresistivity porosity logs were commonly used to calibrate with core porosity to yield the estimate of porosity. The determination of porosity from microresistivity logs depends upon the knowledge of  $R_{xo}$  (formation resistivity) and  $R_{mf}$  (resistivity of the mud filtrate), which responds to the effect of formation that has been flushed with the mud filtrate displacing the connate water with a minimum amount of residual oil saturation in the pore space. Constant cementation exponent,  $m$  is usually used to calculate the porosity and water saturation as derived from the well logs for a given type of rock.

In a heterogeneous formation with different facies and rock types, using a constant  $m$  value for calculation may lead an inaccurate calculation of porosity as well as water saturation. A calibration model was developed accordingly to correlate the porosity of core plugs with well log interpretations to obtain reliable porosity predictions. The model relies on using the variation of  $m$  (cementing exponent) in reference to its relationship with pore geometry classified either by the rock fabric number (RFN) in carbonate rock and flow zone indices (FZI) in sandstone rock. The detailed discussion of the concepts and results is included in Teh's thesis (Teh, 2012) and summarized in the next section.

## **2.2 Improved Geological Model**

The Ogallah unit is a mature oil field produced primarily from the Arbuckle in the early 50's. There are 121 well logs from the wells in the field. The field database contained pre-60's

gamma ray, resistivity and micrologs from most wells. Only one infill drilled well was logged with modern gamma-ray, resistivity and neutron-density log in year 2000. In the RPSEA project completed in 2010, there were no core data available to assist in developing the reservoir description. A primitive geological model was developed based on limited interpretation of well logs with a cross-plotting method. Subsequently, the discovery of core analyses from 18 wells drilled in the Ogallah unit provides a better picture of reservoir lithology, and the opportunity to develop an integrated methodology classifying electrofacies to estimate porosity as well as permeability from logs.

From the lithology description presented in the core analysis report, the upper carbonate sequence (Arbuckle) was found to form a few streaks of dolomite-sand with variable thickness of crystalline-dolomite. The lower Precambrian sequence of the reservoir was deposited with Reagan sandstone. There were 408 core samples from eighteen cored wells. The core plugs were measured with porosity, permeability and saturations at an average sample interval of 0.5 feet and categorized based on the rock type of either dolomite or sandstone without comprehensive classification of pore structures and rock fabrics.

In a routine formation evaluation, cementation exponent  $m$  is usually considered constant for a given rock type to calculate the porosity and water saturation as derived from the well logs. In the work of Focke and Munn (1987), variable values of  $m$  were demonstrated with distinction made between detailed rock types where the  $m$  value depends on grain type and size, pore type and size, and angularity of grains. It is apparent that using a constant  $m$  value for a heterogeneous formation may lead an inaccurate calculation of porosity as well as water saturation. Lucia et al. (2007) proposed a method to estimate the cementation exponent  $m$  based on the pore space description with particular focus on touching and separate vugs. He proposed a continuum of petrophysical classes called rock-fabric numbers (RFN) based on grain size, crystalline structure, sorting and type of pore space and used a visual description of carbonate pore space to classify porosity-permeability relationships. Amaefule et al. (1993) proposed a method of petrophysical relationship zoning based on the flow zone indicator (FZI). In general, the cementation exponent was found to have an inverse relationship with the permeability of sandstone. Frailey et al. (2011) also used groupings of cementation exponent  $m$  to separate the porosity-permeability plot into zones of characteristic  $m$ . Based on the work from these various researchers, the sample classifications of 408 rock samples from 18 wells in the Ogallah unit

were conducted with petrophysical classifiers RFN for carbonate and FZI for sandstone petrophysical classification.

### 2.2.1 Arbuckle Carbonate Classification

The 18 cored wells are located at lease 1, 6, 7, 10 and 11, which are in the west, central east and southeast part of the field. More than 400 core samples were analyzed. Carbonate rocks are classified using the Lucia (1983) rock fabric classification scheme that separates the porosity-permeability data into different classes based on the pore size distribution and interconnectivity. Figure 1 presents the crossplot of log permeability versus porosity of the Arbuckle dolomite overlaid with Lucia classification. The RFN values are calculated from the core measurements of permeability and porosity using the following equation proposed by Lucia (2007)

$$\log(k) = [A - B * \log(rfn)] + [C - D * \log(rfn) * \log(\phi)]$$

Where A=9.7982, B= 12.0838, C= 8.6711 and D= 8.2965.F

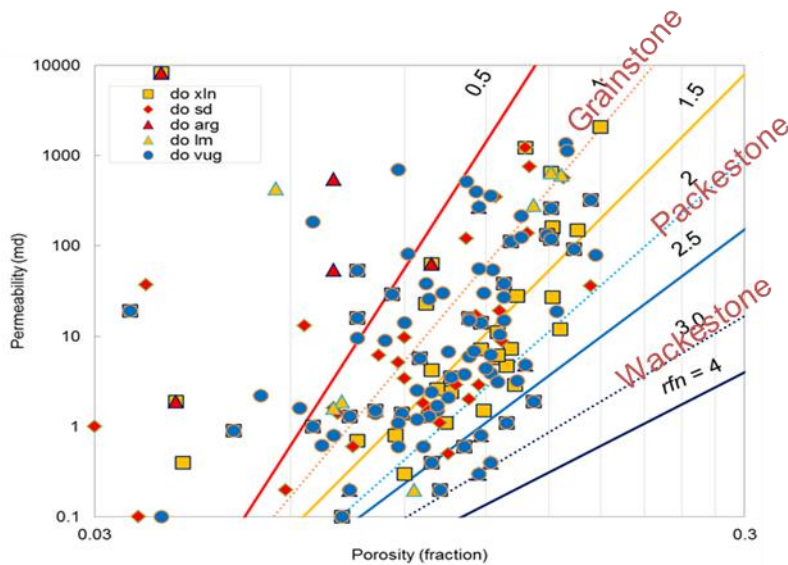


Figure 2: Crossplot of permeability vs. porosity of the Arbuckle dolomite core samples from the Ogallah unit. (Teh et al., 2011)

As shown on Figure 1, each data point represents a measurement of petrophysical properties of core plugs from all the 18 cored wells. The data are scattered, typically seen in carbonate reservoirs. They are grouped into four categories, RFN from 1 to 4 and most of the rock samples fall in the categories of grainstone and packstone. The data then were classified into individual petrofacies groups and the representative m values were calculated for each

group. Table 1 shows the cementation factor for three classes of petrofacies and corresponding mean RFN values with the number of samples in each group considered.

**Table 1: Cementation m and mean RFN values**

Petrofacies	Cementation exponent m	Mean RFN	No. of samples
Outliers	1.319	0.151	25
Grainstone	1.666	0.790	92
Packstone	1.828	1.816	68
Mudstone	1.864	2.842	15

The relationship between m and RFN is plotted in Figure 2 and is represented by the equation

$$m = 0.1883 * \ln(RFN) + 1.6807$$

where m is found to increase linearly with the natural logarithm of rock fabric number (RFN).

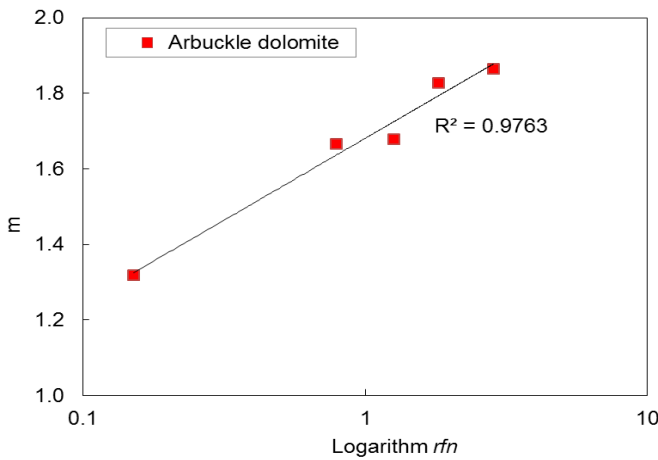


**Figure 3: Relationship between m and Log RFN of the Arbuckle dolomite samples from the Ogallah unit. (Teh et al., 2011)**

### 2.2.2 Arbuckle Sandstone Classification

Sandstone was classified using the FZI as proposed by Amaefule et al. (1993) with the equation

$$FZI = 0.0341 * \sqrt{\frac{k}{\phi^3}} * (1 - \phi)$$

The core data are plotted in Figure 3 with calculated FZI values. The cementation factor values were calculated with the equation as proposed by Salem et al. (1999)

$$m = 2.43 + 0.0316 * \ln(k) + 0.797 * \ln(\phi)$$

Table 2 shows the cementation factor for seven groups of facies and corresponding mean FZI values with the number of samples in each group considered. A strong linear correlation is observed between FZI and the cementation factor  $m$  for sandstone. As shown in Figure 4, the  $m$  values are increased linearly with FZI on a log scale indicating a strong dependency of the cementation factor on porosity.

**Table 2: Cementation factor  $m$  and mean FZI**

FZI	Cementation exponent $m$	Mean FZI	No. of samples
18	1.898	16.892	33
6	1.984	9.101	102
3	1.708	4.466	61
1.5	1.661	2.081	48
0.75	1.594	1.015	45
0.375	1.582	0.544	25
0.1407	1.425	0.222	12

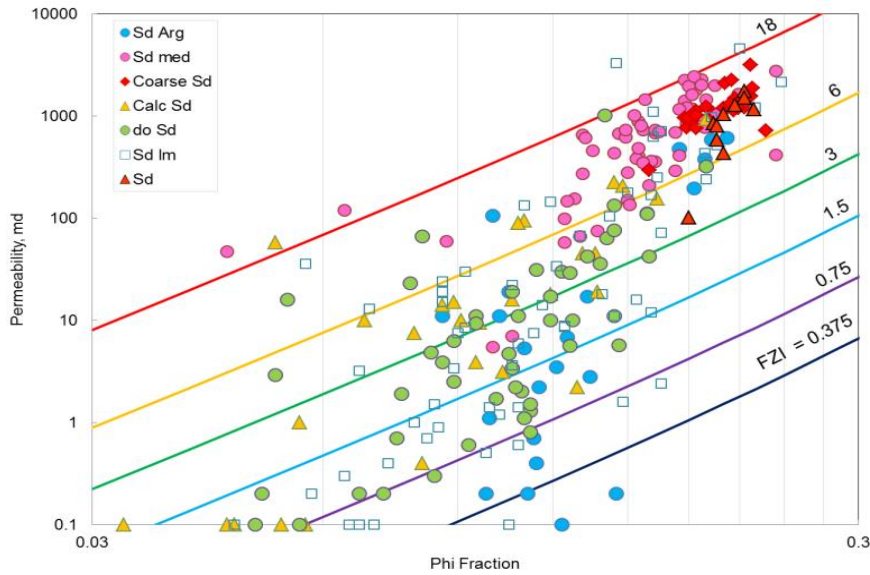


**Figure 4: Crossplot of porosity and permeability of sandstone core samples from the Ogallah unit. (Teh et al., 2011)**

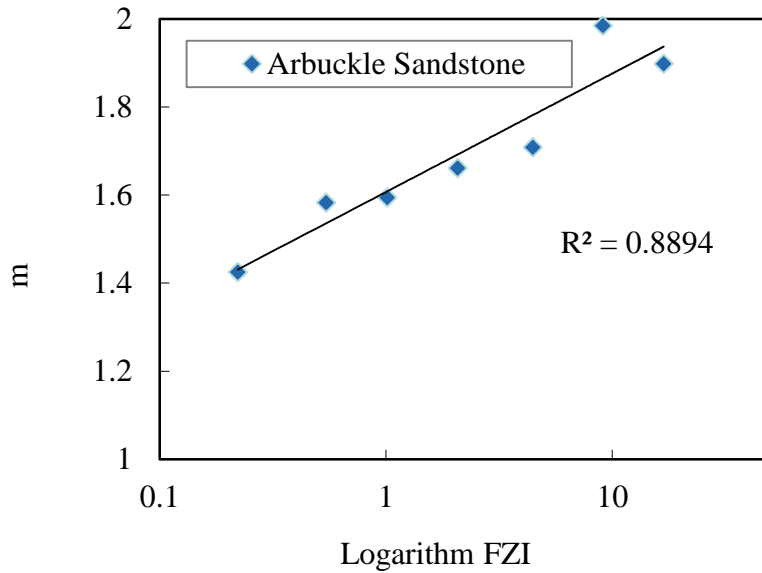


**Figure 5: Relationship between m and FZI of Arbuckle sandstone. (Teh et al., 2011)**

The linear relationships observed between the petrophysical classifiers RFN/FZI and the average cementation exponents m indicate a clear correlation between m values and petrophysical classifiers in the wells with core data. In addition, when all the carbonate core data were separated into clusters using the mean clustering method with gamma-ray and resistivity ratios as the predictors, clusters represent closely the petrofacies and electrofacies as identified on the well logs. Figure 5a shows the clusters with the lithofacies as described in the core analysis while Figure 5b shows four distinct electrofacies groups identified from the well log measurements of the carbonate interval. By a similar approach, the sandstone core data were also separated into clusters as described in the core analysis. As shown on Figure 6a, there are eight clusters representing distinct electrofacies groups. All the data fall in the zone of FZI values between 0.375 and 18 (Figure 6b).

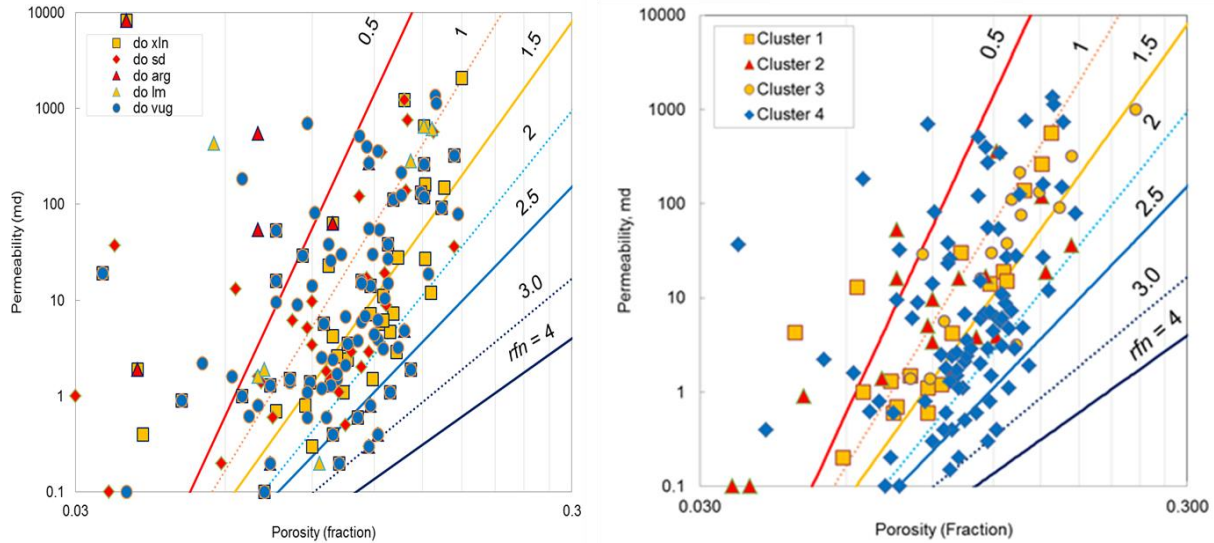


**Figure 6a (on the left) The lithofacies defined by the core, Figure 5b (on the right) corresponding electrofacies identified from the well logs in carbonate. (Teh et al., 2011)**

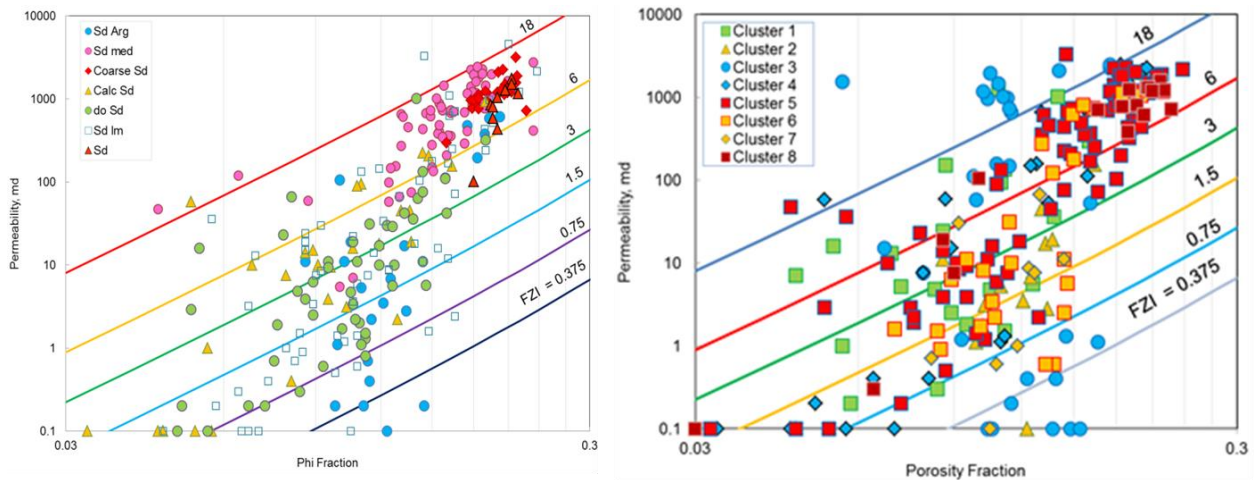


**Figure 7a (on the left) The lithofacies defined by the core, Figure 6b (on the right) corresponding electrofacies identified from the well logs in sandstone. (Teh et al., 2011)**

Based on these observations, it was concluded that clusters of well log measurements display similar trends to the grouped core data according to description of lithofacies by the core analyses. In other words, the lithofacies from core analyses are equivalent to the electrofacies identified from the well log measurements. Subsequently, the transform models were used to correlate well log measurements with petrophysical classifier RFN or FZI to estimate cementation exponent,  $m$  within each electrofacies.

The porosities calculated with the new variable  $m$  values derived from the well logs proved to be much better correlated with the core data as compared to ones determined with a constant  $m$  value. As shown on Figure 7a and 7b, the open circles represent the measured porosities, the black dotted line represents porosities estimated from microlog with a constant  $m$  value, and the blue solid line represents porosities estimated from log with variable  $m$  values derived from the proposed method.

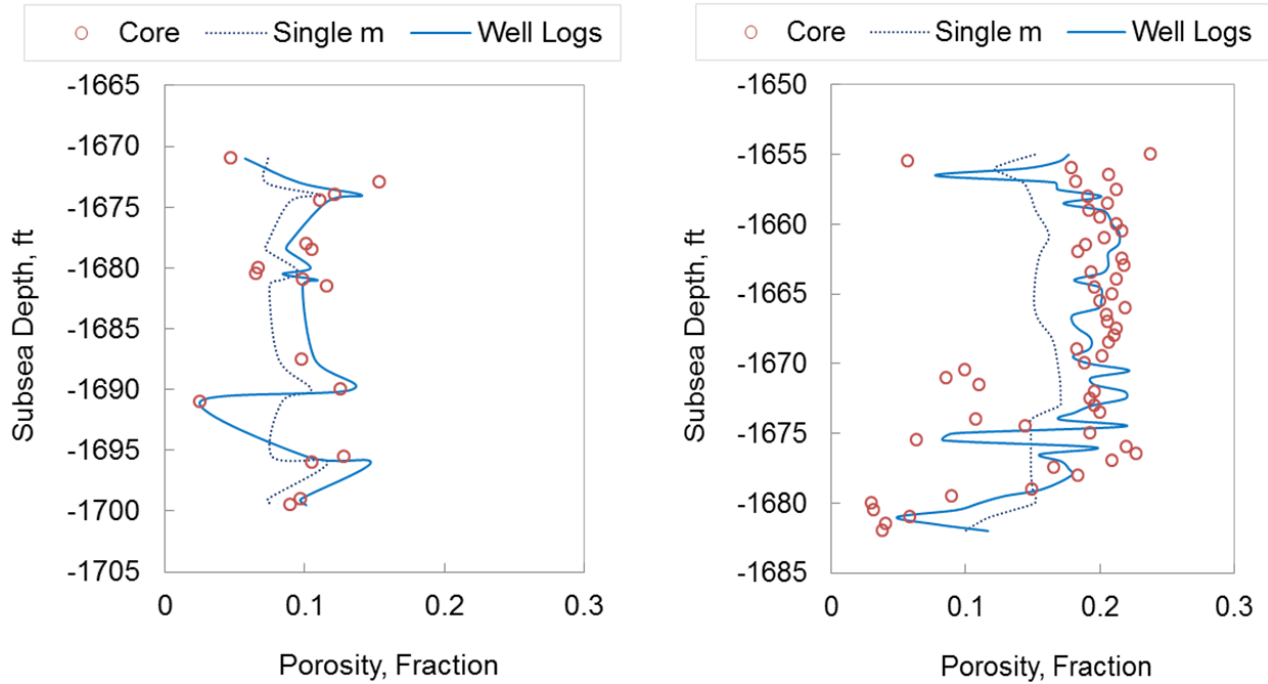


**Figure 8: Comparison between porosity estimation based on constant  $m$  value and variable  $m$  values in carbonate (on the left) and in sandstone (on the right). (Teh et al., 2011)**

This methodology to predict permeability by incorporation of the petrophysical classifiers within electrofacies at well locations also shows improvement of estimation over the simple linear fit for permeability prediction. Figure 8 presents the direct permeability estimation through the correlation of crossplot of permeability and porosity as well as the estimation by incorporation of FZI in the sandstone formation. A better prediction of permeability is observed as the  $R^2$  improved from 0.53 (the plot on the left hand side) where the permeabilities are calculated by direct linear fit to 0.62 (the plot on the right hand side) when the permeabilities are calculated with the improved method. Similar results (see Figure 9) are also observed in carbonate formations where  $R^2$  was improved from 0 to 0.32 when the improved method was used to estimate the permeability.

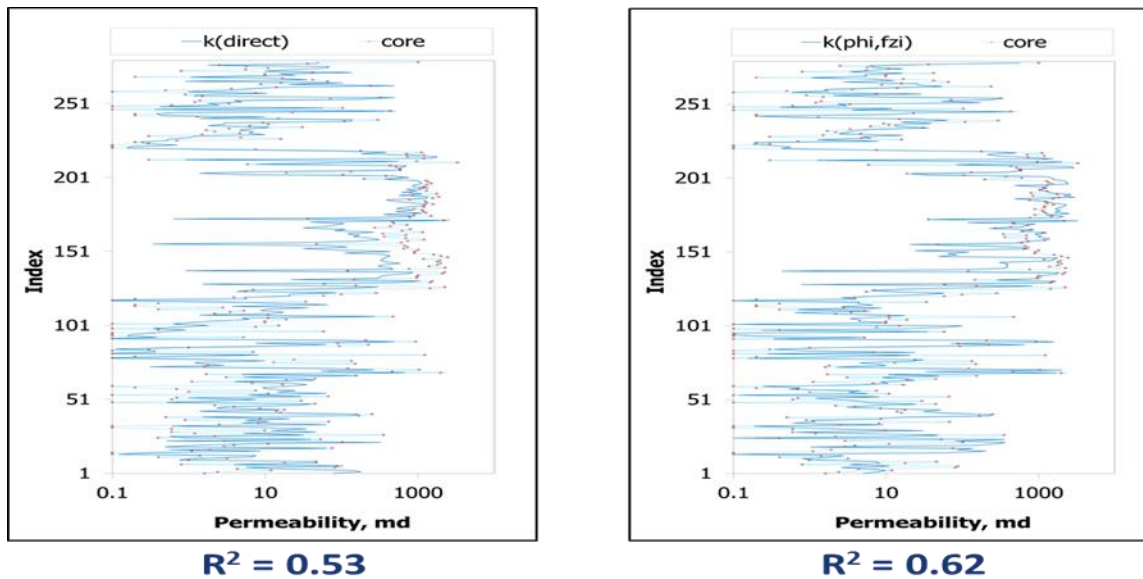


Figure 9: The permeability prediction by using linear fit calculation (on the left) and electrofacies with petrophysical classifier (on the right) in sandstone. (Teh et al., 2012)

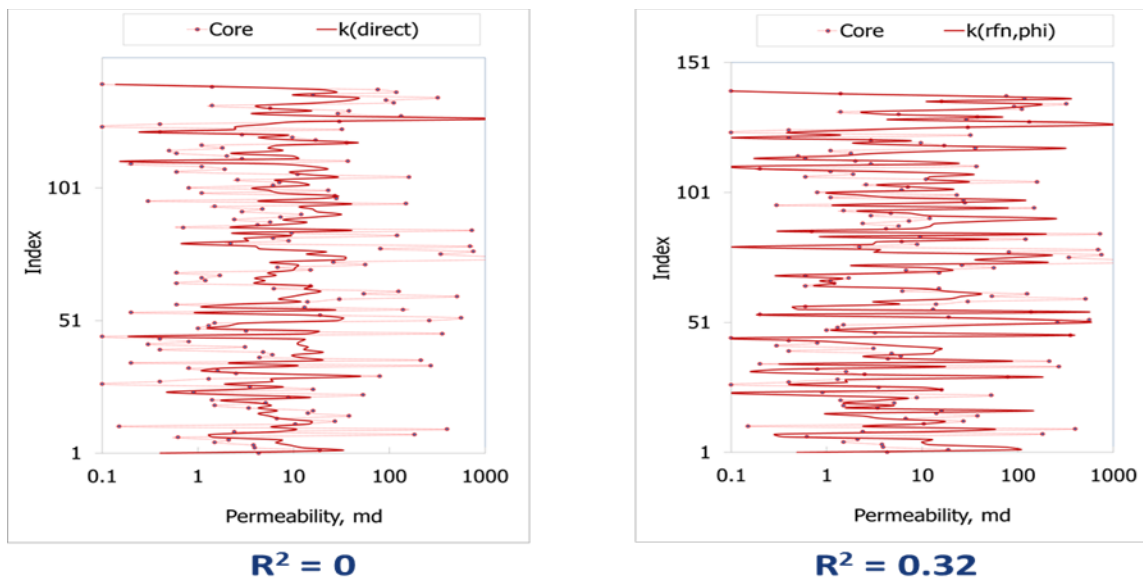
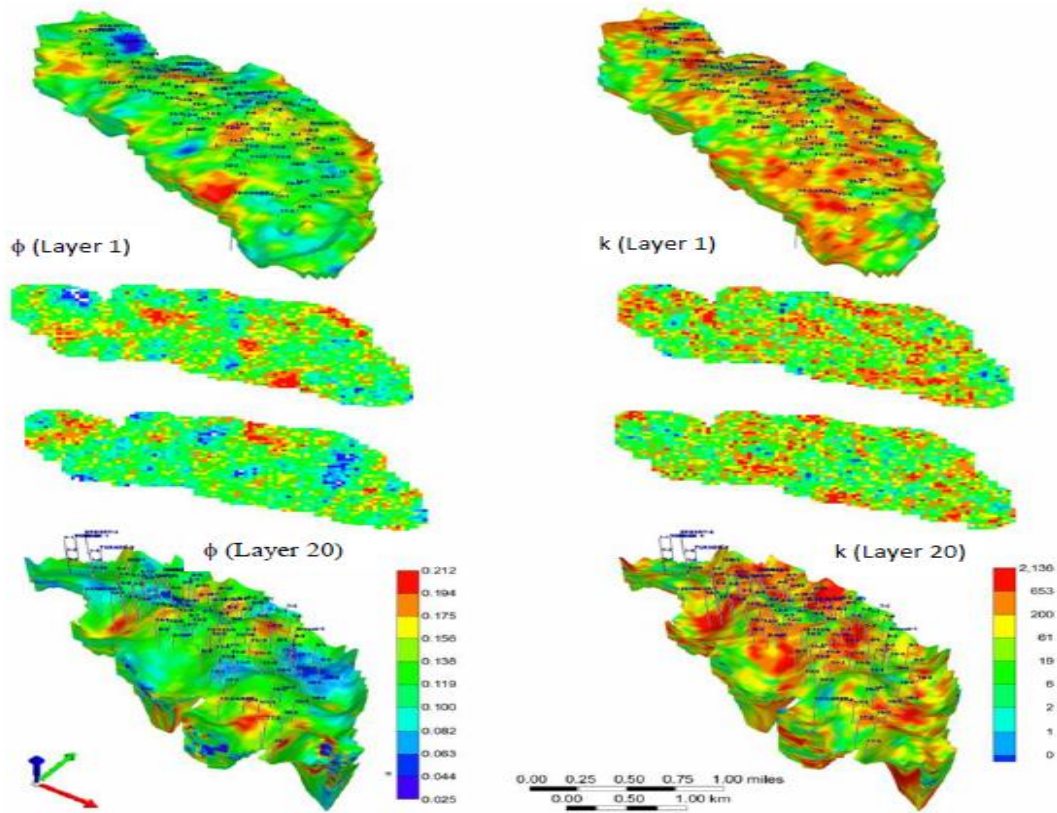


Figure 10: The permeability prediction by using linear fit calculation (on the left) and electrofacies with petrophysical classifier (on the right) in carbonate. (Teh et al., 2012)

The porosity and permeability profile at each well location were generated by the aforementioned improvement of characterization method. Finally, the porosity and permeability were populated using Sequential Gaussian Simulation (SGS) to describe the reservoir of the Ogallah unit. Figure 10 presents the porosity and permeability distribution of layer 1 and 20.

The red color on the property scale represents high values of porosity and permeability whereas blue color represents low values of the property and green is used for values in between.



**Figure 11: Porosity and permeability distribution of the Ogallah field. (Teh, 2012)**

Based on this geological model, the Ogallah unit is described as two production units, an upper unit of Arbuckle dolomite consisting of the top 20 layers in the model and a bottom unit of Reagan sandstone consisting of another 20 layers. The range of the porosity is between 0.1 and 0.15 and the permeability varies from 0.54 md to 3750 md.

### 2.3 Reservoir Model

The reservoir model was discretized with 100 blocks in the east-west direction, 60 blocks in north-south direction and 40 layers in the vertical direction. The grid block size was 220 feet in width and length with variable thickness in layers. Excluding the null blocks, the grid system consists of 101,100 active grid blocks. Figure 11 presents the structure top of the field in depth below subsea level. The structure high is in the center portion of the field at least 4 and 7. Figure 12 shows an example cross-section view of the layers consisting of Arbuckle dolomite

(blue color) and Reagan sandstone (magenta color). The reservoir was modeled with an underling aquifer by means of the Carter-Tracy method to simulate the mechanism of bottom water drive.

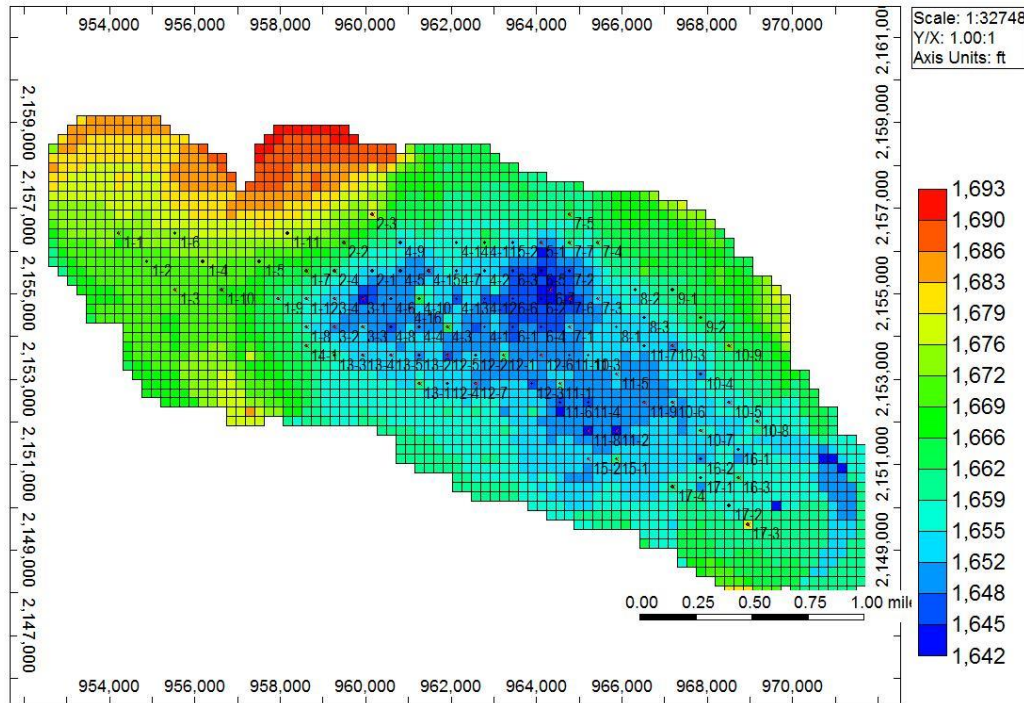


Figure 12: Structure top of Ogallah unit (subsea level)

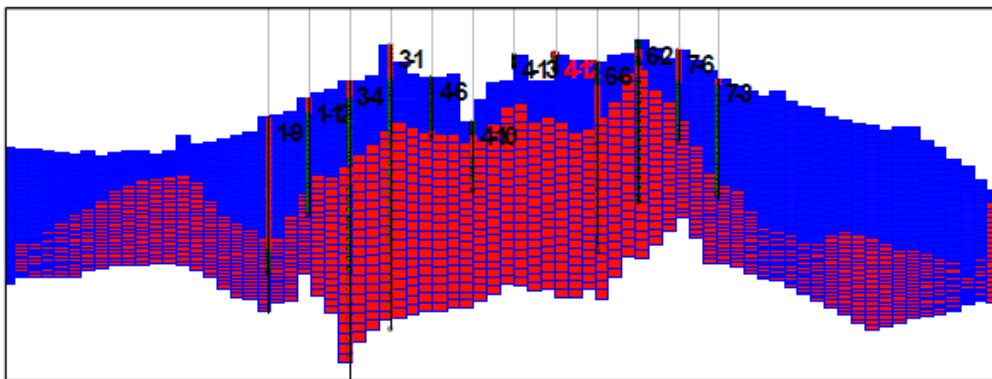


Figure 13: Example cross-section view of Ogallah unit. (Teh, 2012)

## 2.4 Production History

Primary production of the Ogallah started in 1951. Well production history shows that no water was produced before 1960. Water breakthrough in producers started after 1960. Due to

the high water production, wells were worked over with well deepening, formation plug-back and perforation at upper intervals. At the peak of production in 1969, the Ogallala field had 85 producing wells. The field was producing 1.07 MMBO/year with cumulative production of 11.37 MMBO by 1969. After 1969, the field commenced commingled production from the Lansing-Kansas City formation (LKC) and half of those wells were shut in by 1989 due to economic decline. The Ogallala field was unitized in 1991 and the number of active producers since then was reduced to 18.

Figure 13 shows the field map with 103 wells located in 18 leases. Dark green dots represent 13 current active producers completed in the Arbuckle formation only; light green dots represent other active producers with comingled production including the Arbuckle formation; yellow dots and orange dots represent temporarily abandoned wells.

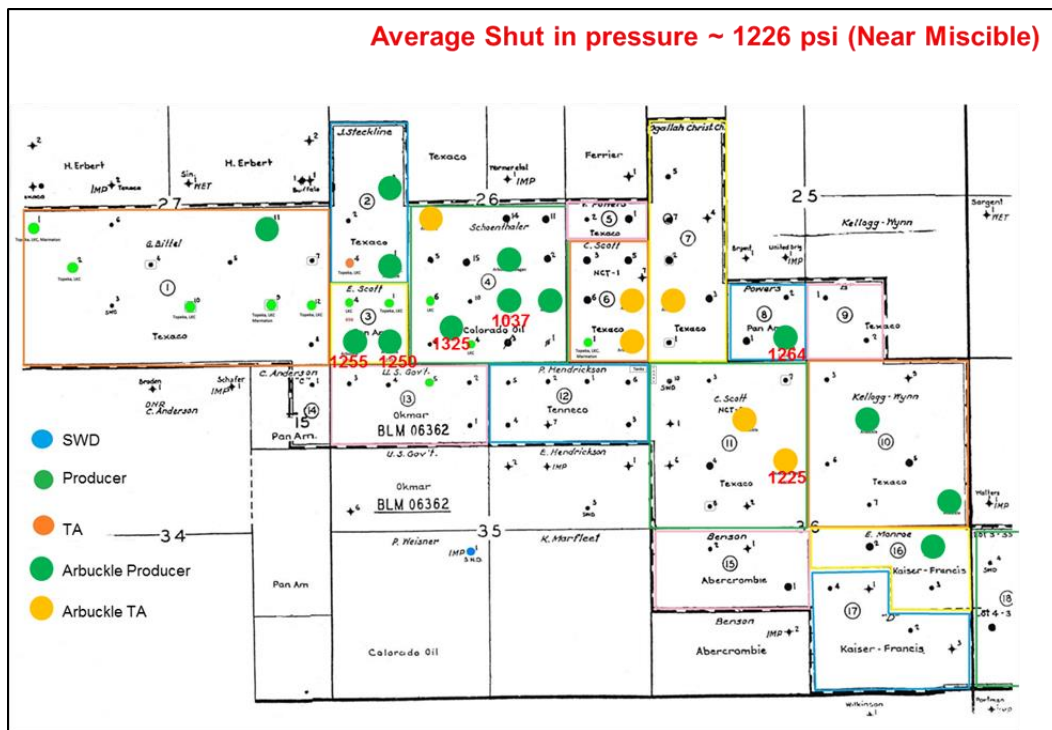


Figure 14: Map of lease boundary and well locations.

Individual well production history in the Ogallala unit was not recorded in the early years of production. The most recent record for individual active producers was from 1991 onwards and most producers are in comingled production. Figure 14 shows the production history of Lease 3 where the production started in 1952 when well 3-1 and 3-2 were first drilled and produced from the Arbuckle. Well 3-3 started production from the Arbuckle in 1955. The total

production rate from all three wells stabilized at around 2700 BO/month. The production rate started to decline from 1963. In 1965, well 3-4 was drilled and produced from the Arbuckle and Lasing-Kansas City (LKC). In late 1965, the LKC-F zone was perforated in well 3-1 to have comingled production with the Arbuckle. The production rate started to decline significantly after water breakthrough. Another apparent rate increase occurred in 1977 when well 3-1 was perforated in the LKC-A and Topeka. The Arbuckle production of the Ogallah unit is primarily attributed to natural water drive as the reservoir pressure has been maintained at around 1150 psi for more than 50 years. In a recent pressure measurement on wells as shown on Figure 13, an average shut-in pressure of lease 3 and the field were 1252 and 1226 psi, respectively, which fall in the range of near miscible pressure as determined from the laboratory experiments. (Ly, 2010).

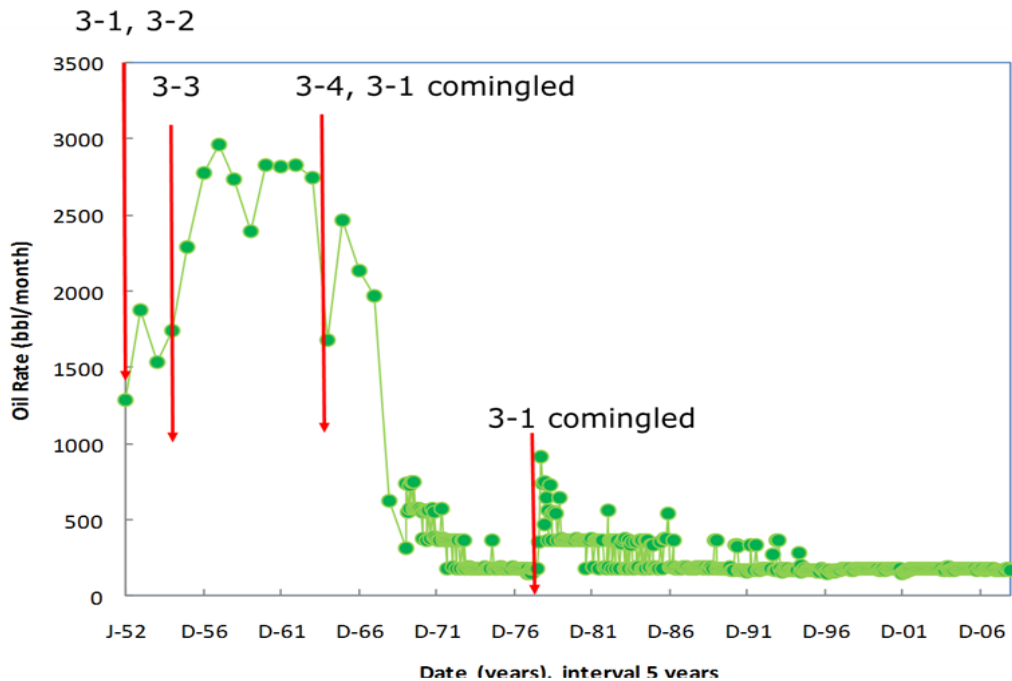


Figure 15: Annual production history of Lease 3. (Tsau, 2010)

## 2.5 Primary Production Simulation

To simulate the primary production by bottom water drive, a black oil simulator, CMG's IMEX, was used to history match the production performance on the leases. The Carter-Tracy method was implemented to model a bottom water drive aquifer. The volumetric performance of reservoir fluids at various pressure levels are tabulated in Table 3. These data are derived from the laboratory studies of PVT of reservoir fluid in a previous report. (Tsau, 2010)

**Table 3: PVT data used in black oil simulator**

P	Rs	Bo	z	viso	visg
(psia)	(scf/stb)	(rb/stb)		(cp)	(cp)
15	3.5	1.021	0.999	4.124	0.0124
412	62.8	1.039	0.964	2.906	0.0127
809	136.7	1.063	0.933	2.176	0.0133
1206	218.6	1.091	0.908	1.735	0.0140
1603	306.1	1.122	0.889	1.445	0.0148
2000	398.1	1.157	0.878	1.241	0.0157

Figure 15 shows the oil-water relative permeability curves used in the simulation. The relative permeability was modeled using modified Corey-type equations (Corey, 1954) where  $S_{wc}$  was obtained from the laboratory measurement. The modified Corey relative permeability equations used were:

$$k_{ro} = k_{ro_{S_{wi}}} (1 - S_{WD})^n$$

$$k_{rw} = k_{rw_{S_{ORW}}} (S_{WD})^m$$

$$S_{WD} = (S_w - S_{WC}) / (1 - S_{ORW} - S_{WC})$$

where  $n$  is the exponent of the oil relative permeability and  $m$  is the exponent of water relative permeability. The  $m$ - and  $n$ -exponent used are 5 and 2 respectively. The end-point residual oil and water saturation are both 0.25.  $k_{ro_{S_{wi}}} = 1.0$ ;  $k_{rw_{S_{ORW}}} = 0.18$ .

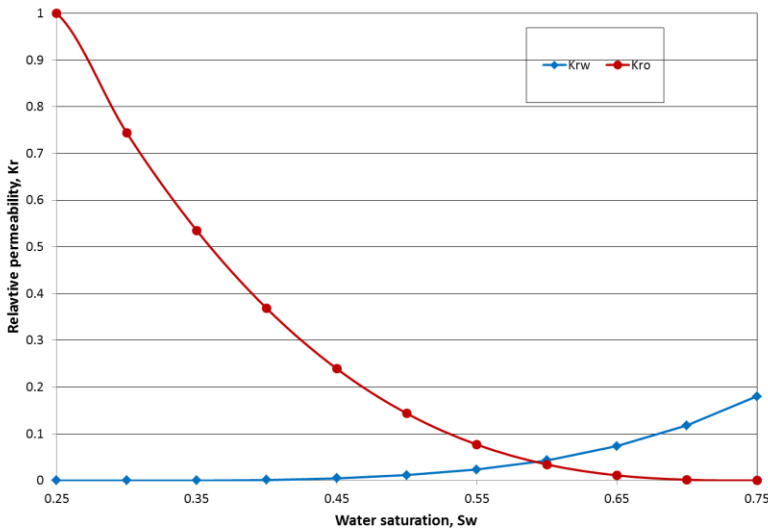


**Figure 16: Relative permeability curves of oil and water for dolomite and sandstone in simulation.**

The initial reservoir pressure was assumed to be 1200 psia based on DSTs conducted in the early years of production. The rate constraint was applied to the wells when prorated production before 1970 was imposed. Otherwise, the pressure constraint was applied to the producers at a given bottomhole pressure when the record was available or pumped off when it was not available.

The history match was performed to match the simulated production results with lease production history. Although the unit has been in production since 1951, the average reservoir pressure was not changed significantly, as the pressure was supported by the underlying aquifer. Figure 16 shows the calculated average reservoir pressure decreasing from 1200 psi to 1190 psi for the whole field and to 1185 psi for the lease 3 in 50 years of production. This indicates that the Carter-Tracy method is adequate to simulate the pressure support as needed by the reservoir performance.

The reservoir description and recovery mechanism with natural water flood by the underlying aquifer are also verified by evaluation of WOR behavior in individual wells. Figure 17 shows two examples of reasonably well matched WOR history in well 1-6 and 6-1 where the open circles represent field data and the lines represent simulation results. Figure 18 shows a simulated example of primary production mechanism driven by the aquifer. The oil saturation map as displayed in a cross-section of the Ogallah field shows the movement of water-oil contact (interface between green color and yellow color). As the field was in primary production from 1952 to 2011, the simulator shows that the water-oil contact has gradually risen with the water influx from the underlying aquifer. The effect of permeability stratification influences the observed production history.

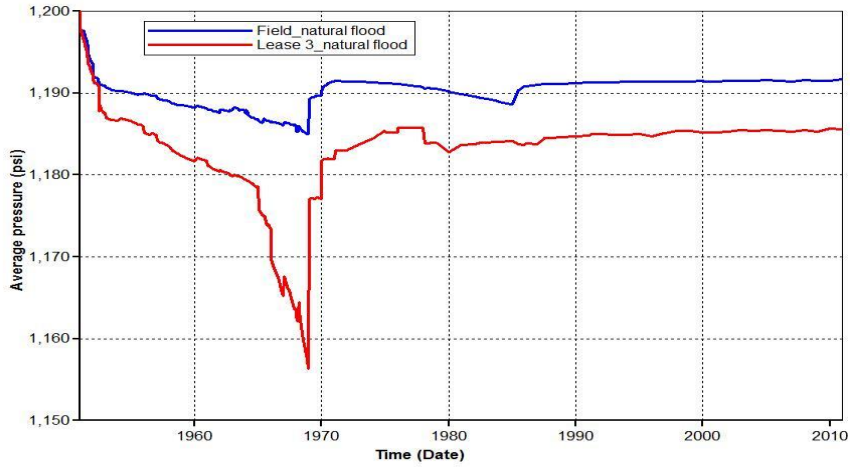


Figure 17: Average reservoir pressure during primary production.

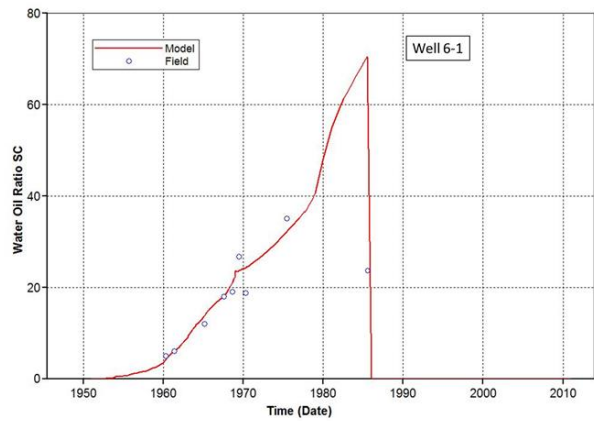
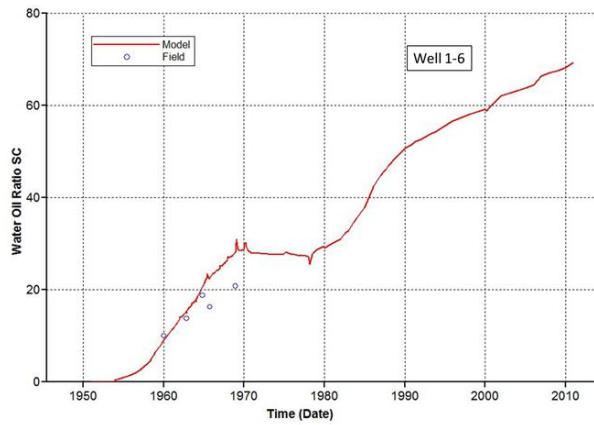
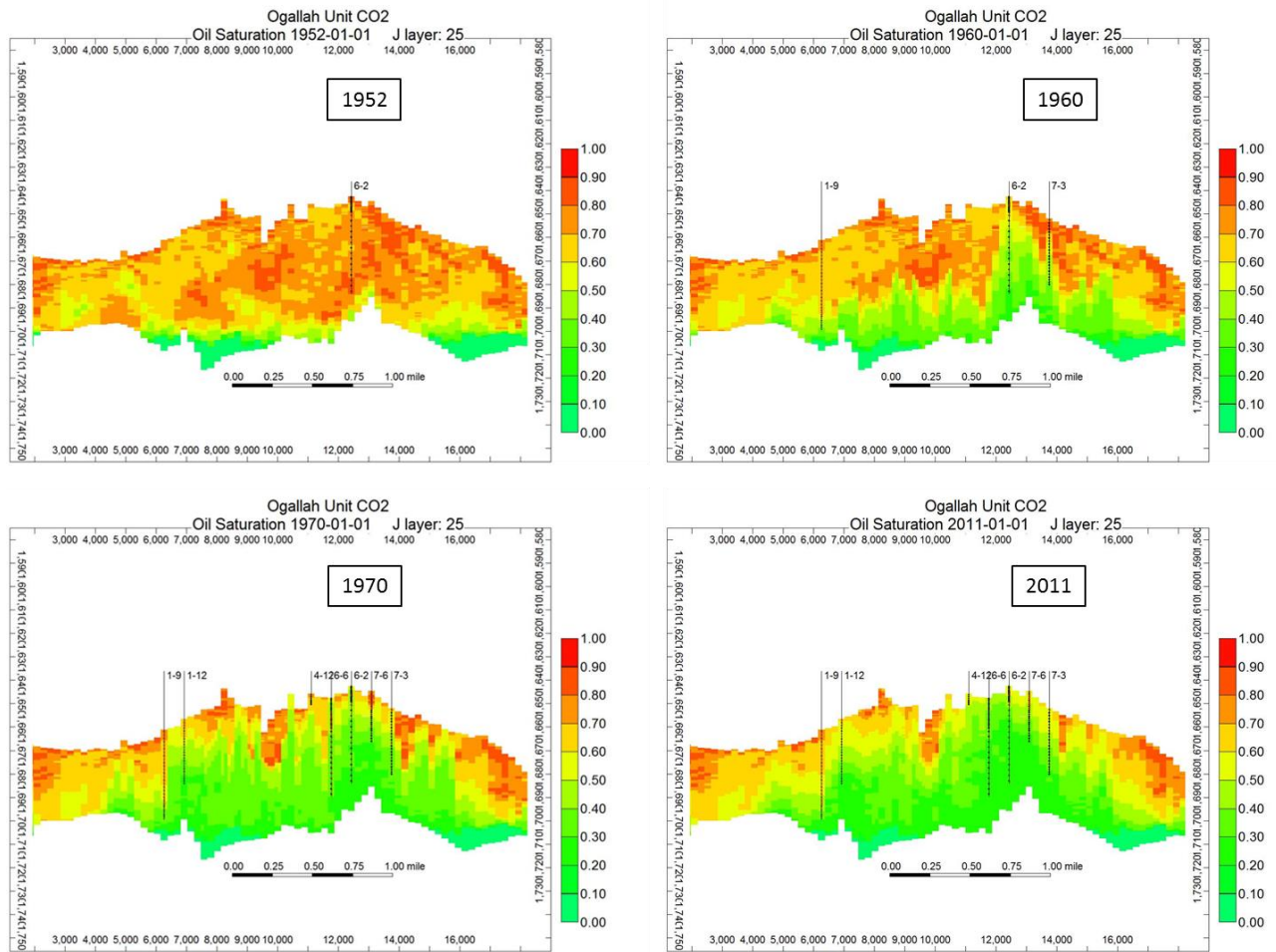
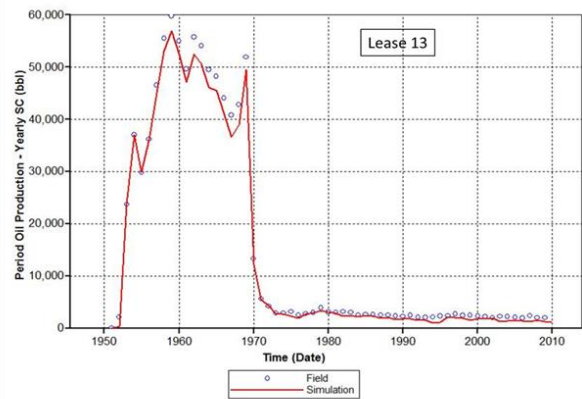
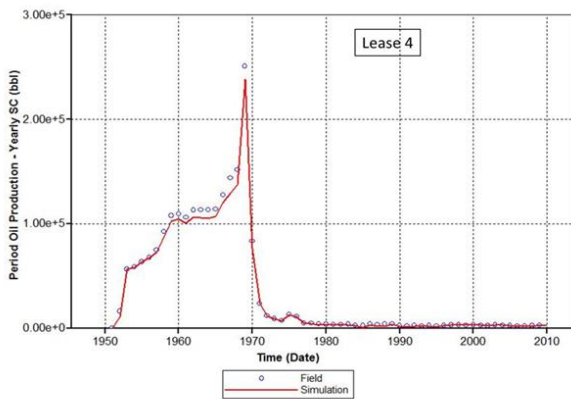
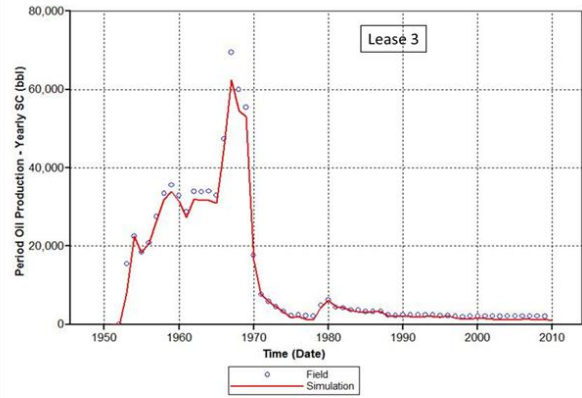
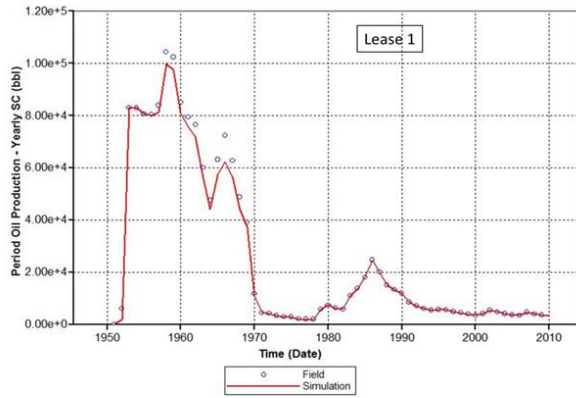


Figure 18: Water-oil ratio history match of well 1-6 and 6-1.



**Figure 19: Simulated movement of water-oil contact during primary production period from year 1952 to 2010.**

When the vertical permeability of each grid is assumed to have equal areal permeability, the lease production history is also reasonably well matched. Figure 19 show the history matched results in four leases where the open circles represent field data and the red lines represent simulation results.



**Figure 20: Lease production history match during primary production.**

The current reservoir model has a better history match on lease productions in the Ogallah unit. Figure 20 shows lease 3 (on the left) and lease 4 (on the right) production history match with two different models. Open blue circles are field production data. The blue curve shows the simulation results with the old model and the red curve with the current model. Although the old model matches production history after 1980, noticeable mismatch exists prior to 1970. The current model is developed through an integrated characterization method and proved to be a better representative model for further reservoir simulation.

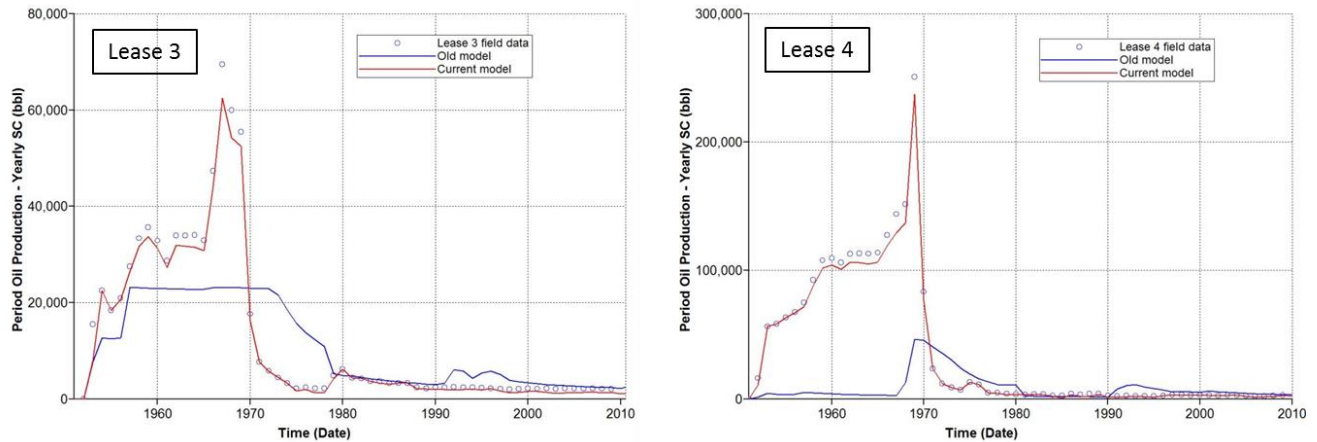


**Figure 21: Comparison of lease production history between models.**

## 2.6 Simulation of Carbon Dioxide Injection

The original research plan to conduct additional tests (such as individual well transient pressure tests, multiple well interference tests and interwell tracer tests) in the Ogallah unit was cancelled due to the withdrawal of participation of the oil field operator. Without these tests, the evaluation plan for better understanding the nature of the flow paths between wells and calibrating the reservoir model for extended simulations on the CO<sub>2</sub> IOR process is compromised. With the revised research plan, nevertheless, the new reservoir model without further calibration was applied in simulation of CO<sub>2</sub> flooding.

In a previous RPSEA report, preliminary modeling results on lease 3 were derived from an old reservoir model where the reservoir properties were characterized with a primitive method. The simulation results in that report shows the oil mobilization is achievable in lease 3 at near miscible conditions. The incremental oil recovery varies with the pattern design and, in general, the oil recovery efficiency is increased as a result of CO<sub>2</sub> injection. With the current reservoir model, similar approaches are applied to investigate the feasibility of CO<sub>2</sub> flooding at near miscible conditions.

Lease 3 is one of the smallest leases in the unit and is located in the central-west part of the field (Figure 13). It is surrounded by lease 1, 2, 4 and 13. The lease has producers 3-2 and 3-3 currently producing from the Arbuckle formation and producers 3-1 and 3-4 with comingled production from the Arbuckle and LKC formations. To model the CO<sub>2</sub> injection process, the black oil model in IMEX for history match was converted to a compositional model in GEM using a four-pseudocomponent equation of state (EOS) to simulate phase behavior of reservoir

fluids and recovery performance during a CO<sub>2</sub> displacement process. Table 4 summarizes the description and input for the equation of state calculations. Predictions of phase behavior with these lumped compositional data have been verified with experimental results in swelling factor, MMP and viscosity of swollen oil. (Tsau, 2010)

**Table 4: Lumped compositional description of reservoir fluid**

Component	Mole fraction	Pc (atm)	Tc (K)	Acentric factor	Molecular weight (g/mol)
CO2	0.0000	72.80	304.2	0.225	44.0
C3-C6	0.0875	33.11	488.5	0.258	79.4
C7-C16	0.6171	24.43	629.7	0.452	140.1
C17-C35	0.2255	12.89	813.9	0.903	312.7
C36+	0.0699	6.93	865.6	1.173	979.8

The relative permeability curve of gas and oil (Figure 21) along with the relative permeability curves of water and oil (Figure 15) are used in the compositional model.

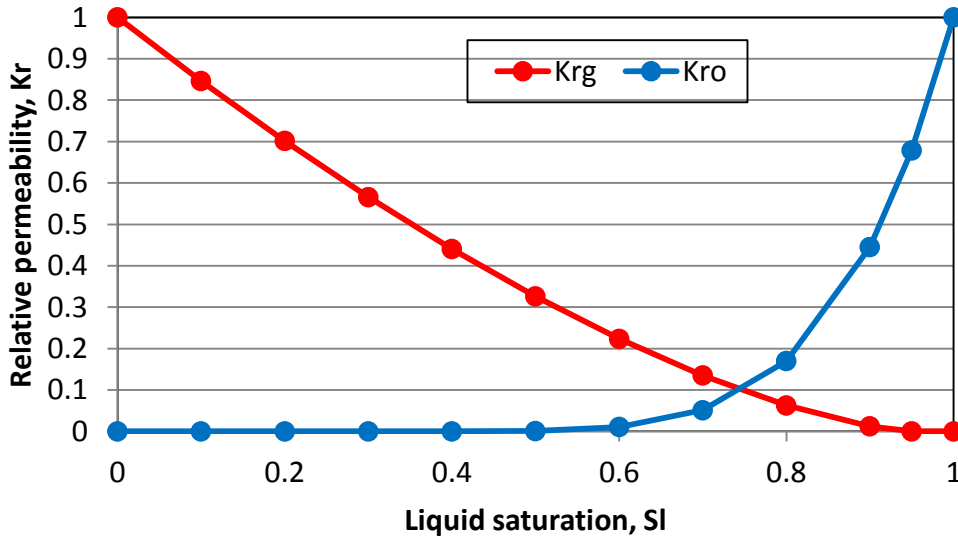


**Figure 22: Relative permeability of gas and oil used in gas injection process.**

Furthermore, the grid in the lease area was refined to better describe recovery processes associated with gas injection. Figure 22 shows the grid system of lease 3 (highlighted in

magenta color grids) with neighboring leases. The cell width and length is refined from 220 ft to 110 ft with variable thickness in layers.

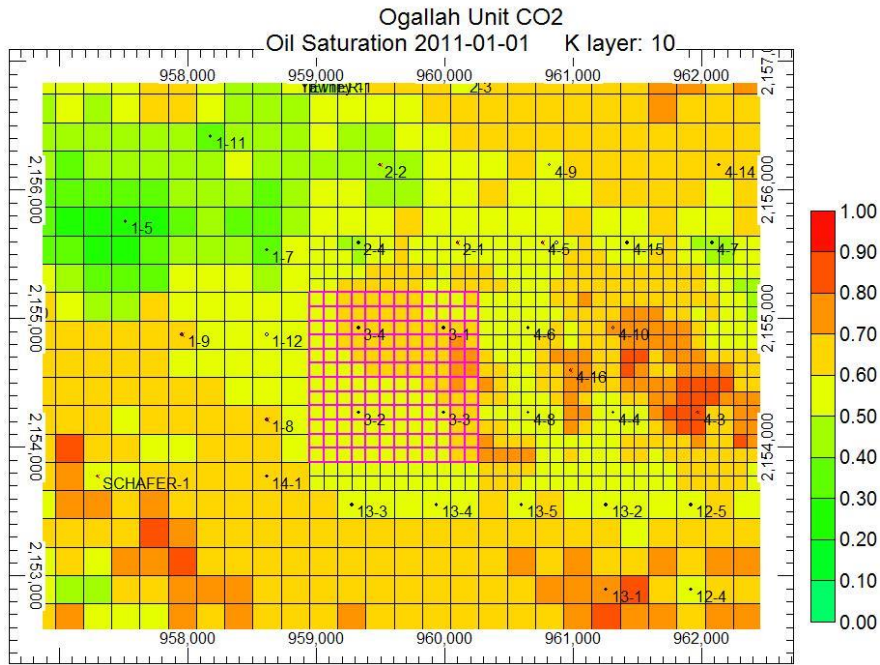


**Figure 23: Grid system of lease 3.**

The pattern design is shown in Figure 23 wherein each pattern consists of two injectors and two producers. In a continuous CO<sub>2</sub> injection case, the injector is shown in red color and injects a constant rate of 200 MSCF/day and producers are shown in green color and produce at a constant bottomhole pressure of 28 psi.

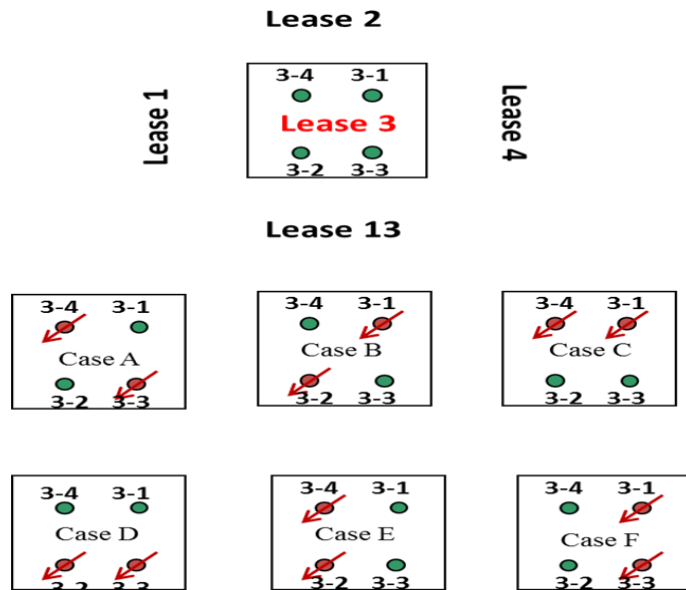


Figure 24: Pattern design in CO<sub>2</sub> injection on lease 3. (Tsau et al., 2010)

The lease primary production prior to CO<sub>2</sub> injection was simulated from January 1951 to January 2011. Then lease production was continued without CO<sub>2</sub> injection until January 2020. In this period, the recovery mechanism of the reservoir depends on the natural water drive from the underling aquifer and the reservoir performance is referred to as a base case.

To investigate the effect of flow path and injection schemes on the performance of oil recovery by CO<sub>2</sub> injection, displacement of CO<sub>2</sub> at near miscible conditions was examined with different scenarios. Figure 24 shows an example of a layered permeability and porosity map generated in the model. The relatively high permeability grid blocks (red and orange colors) are observed sporadically between wells inside the lease.

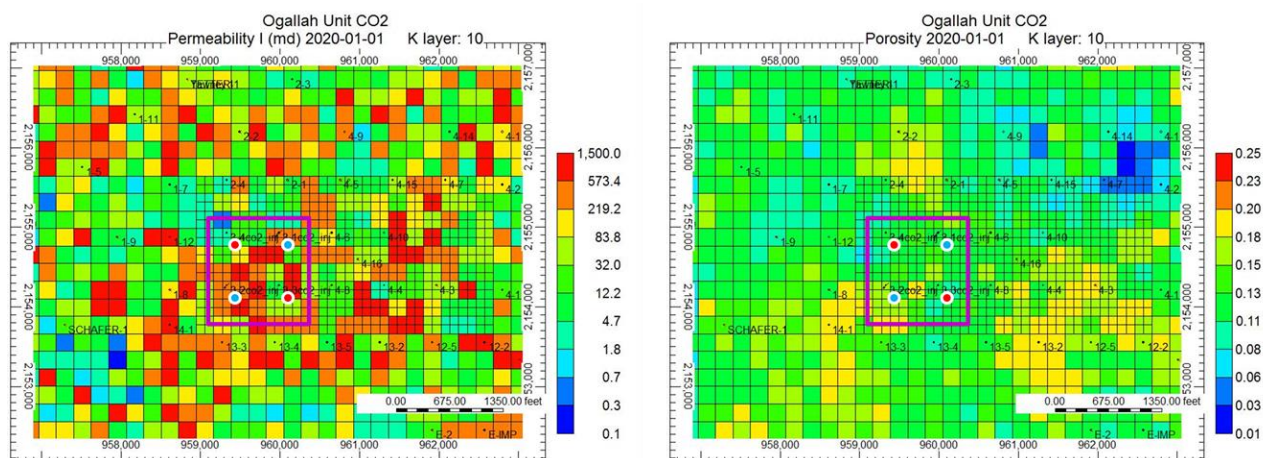


Figure 25: Permeability and porosity map of layer 10.

### 2.6.1 Continuous CO<sub>2</sub> Injection

For continuous injection of CO<sub>2</sub>, a constant rate of 200 MSCF/day is applied in each of the two injectors in the lease. The other two wells produce at a constant bottomhole pressure of 28 psia. The original oil in place (OOIP) of lease 3 at the beginning of primary production is estimated at 1.60 MMSTB with 0.84 MMSTB original water in place (OWIP). After 50 years of primary production, the remaining oil in place prior to CO<sub>2</sub> injection in the lease is 975 MSTB. Figure 25 shows recovery factor and average pressure of lease 3 during the period of primary production and CO<sub>2</sub> injection. The percentage of oil in the lease displaced through a recovery process is defined as oil recovery factor. It is different from the recovery efficiency defined as the percentage of produced oil in a lease. The MMP of the reservoir oil is 1350 psi and the average lease pressure during simulated CO<sub>2</sub> injection increases from 1188 to 1244 psi, which indicates the displacement of oil is under near miscible conditions. The recovery factor increases from 39.2 to 44.8 indicating 5.6 % of OOIP is displaced by the CO<sub>2</sub> injection process.

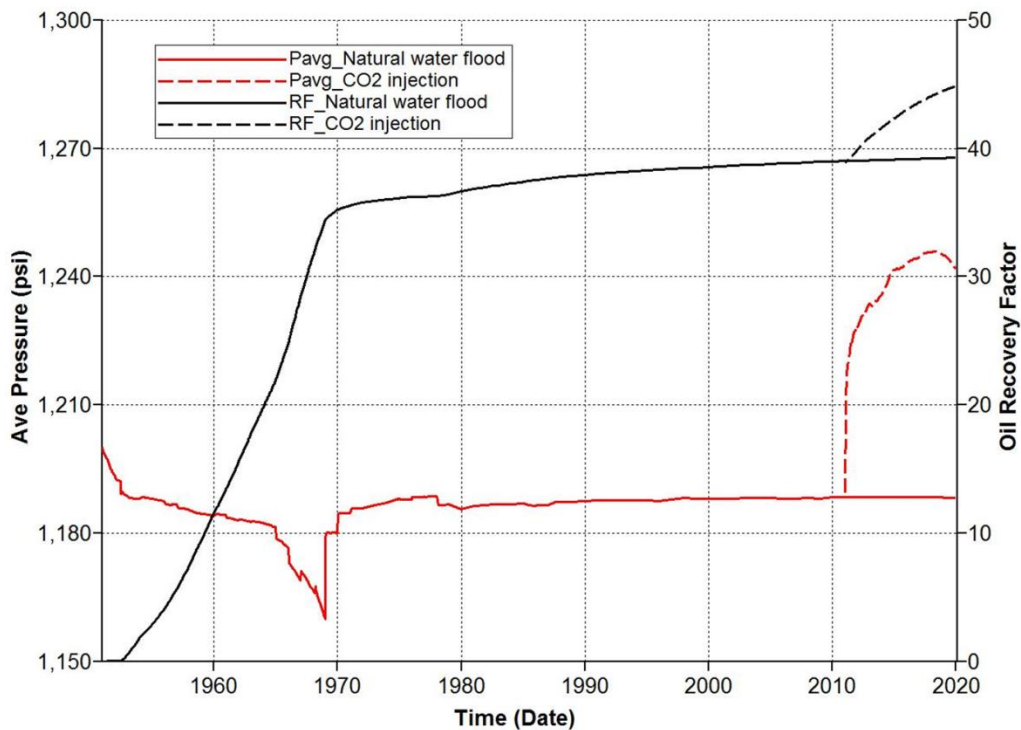
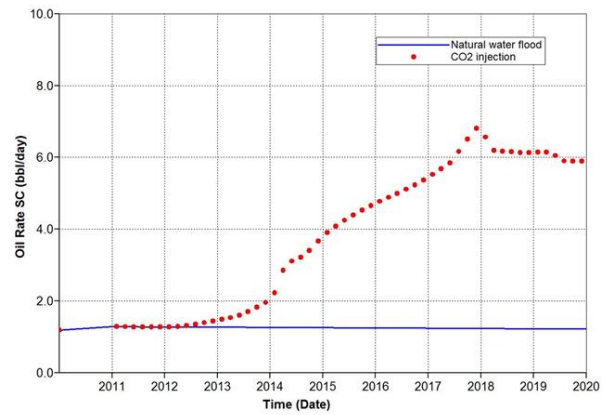
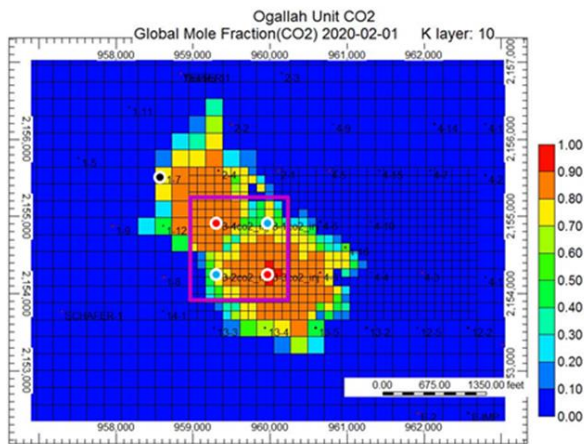


Figure 26: Comparison of recovery factor and average reservoir pressure in case A.

Total volume of CO<sub>2</sub> injection from 2011 to 2020 was 1314 MMSCF, which corresponds to 0.5 PV of reservoir volume in lease 3. As there is no confinement wells in the pattern to confine CO<sub>2</sub> inside the lease during the injection, some of the oil is displaced to the neighboring lease. By examining the CO<sub>2</sub> concentration and oil saturation distribution at the end of CO<sub>2</sub> injection, it appears that some of the lease oil was displaced to other wells at the neighboring leases. Figure 26 shows the production profile of well 1-7 (black dot on the left side of plot) which is located 930 feet northwest of CO<sub>2</sub> injector 3-4. The oil rate produced from well 1-7 increased from 1 to 6.5 bbl/day about two years after inception of simulated CO<sub>2</sub> injection in injector 3-4, which indicates that oil mobilized by carbon dioxide injection on Lease 3 was displaced to Lease 1.



**Figure 27: Production history of well 1-7, which is located 930 feet northwest of CO<sub>2</sub> injector 3-4.**

Figure 27 shows the plot of CO<sub>2</sub> concentration and oil saturation distribution in layer 10 at the end of CO<sub>2</sub> injection. The injectors are represented by red circles while the producers are shown in blue circles. As shown on the map, CO<sub>2</sub> tends to flow along the alignment of injectors. Some of the oil displaced by CO<sub>2</sub> crosses the lease boundary and is produced in the neighboring wells.

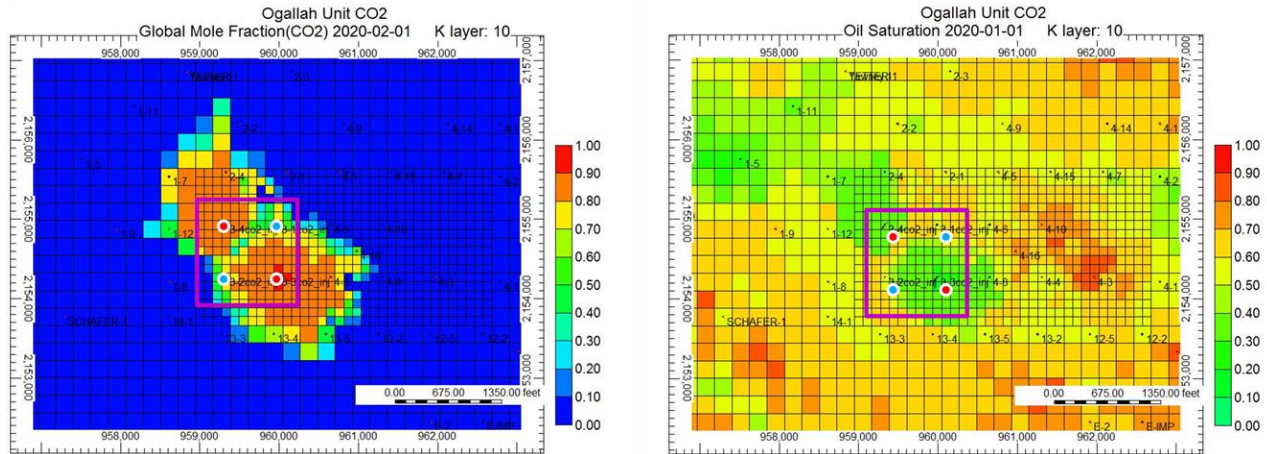


**Figure 28: CO<sub>2</sub> (on the left) and oil saturation distribution (on the right) for injection pattern A, (red circles represent injectors, blue circles represent producers)**

**Table 5: Summary of production and injection results of case A**

CO <sub>2</sub> injected (MMSCF)	1314
CO <sub>2</sub> produced (MMSCF)	95.03
CO <sub>2</sub> remained (MMSCF)	1219
Incremental oil produced from well 3-1 (STB)	1860
Incremental oil produced from well 3-2 (STB)	8911
Incremental oil produced from well 1-7 (STB)	8690
Incremental oil produced from well 2-4 (STB)	1017
Incremental oil produced from well 4-8 (STB)	923
Total incremental oil relative to Base case (STB)	21402
Water production base case (MMSTB)	1.69
Water production case A (MMSTB)	1.28
Recovery factor (displacement efficiency)	44.9
GU (MSCF/STB)	61.4
NU (MSCF/STB)	57.0

Table 5 summarizes the production results of case A from the model calculation. The incremental oil production, 21,402 STB, represents 2.2% of residual oil in place (ROIP) from lease 3. However, 40% of incremental oil production is from the neighboring well 1-7 in this case, which indicates a significant amount of the mobilized oil can be lost to a surrounding lease if the field is not unitized. The gross utilization (GU) and net utilization (NU) of CO<sub>2</sub> are 61.4 and 57.0 MSCF/STB, respectively, which are higher than normally seen in CO<sub>2</sub> miscible flooding applications. Nevertheless, the production of water is reduced when CO<sub>2</sub> is injected as

a displacing agent. A typical reduction of water cut in a producer is commonly seen with the increase of gas-oil ratio in the producer. Figure 28 shows the production performance of well 3-2 during simulated CO<sub>2</sub> injection. The oil rate responds to CO<sub>2</sub> injection and is increased from 1.8 to 2.5 b/d, and to 3 b/d after CO<sub>2</sub> breakthrough. The water cut is reduced from 0.9 to as low as 0.04. Similar behavior of CO<sub>2</sub> flowing pattern is observed in other injection patterns. As seen from Figures 29 to 33, high CO<sub>2</sub> concentration and low oil saturation are displayed along with the alignment of injectors.

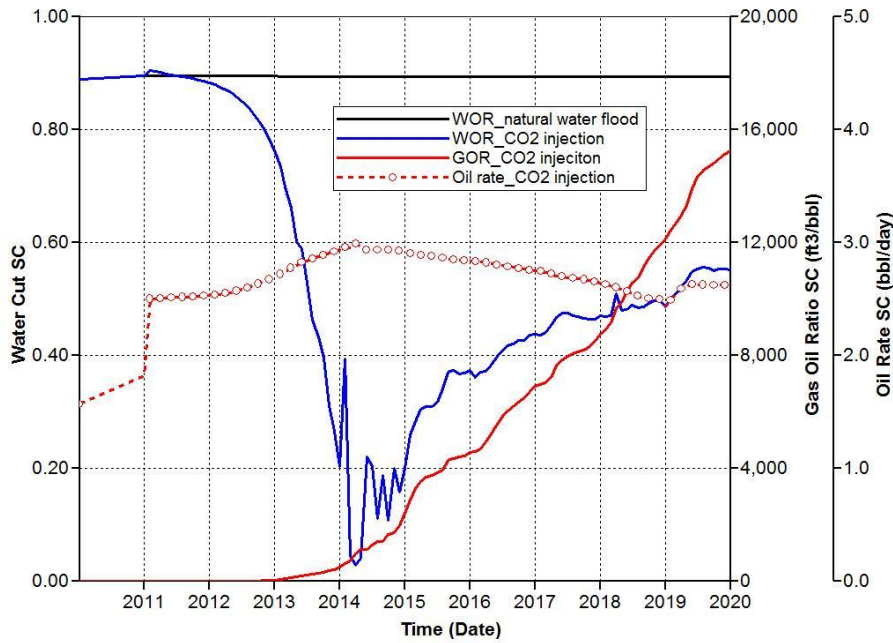


Figure 29: Production performance at producer 3-2 during simulated CO<sub>2</sub> injection.

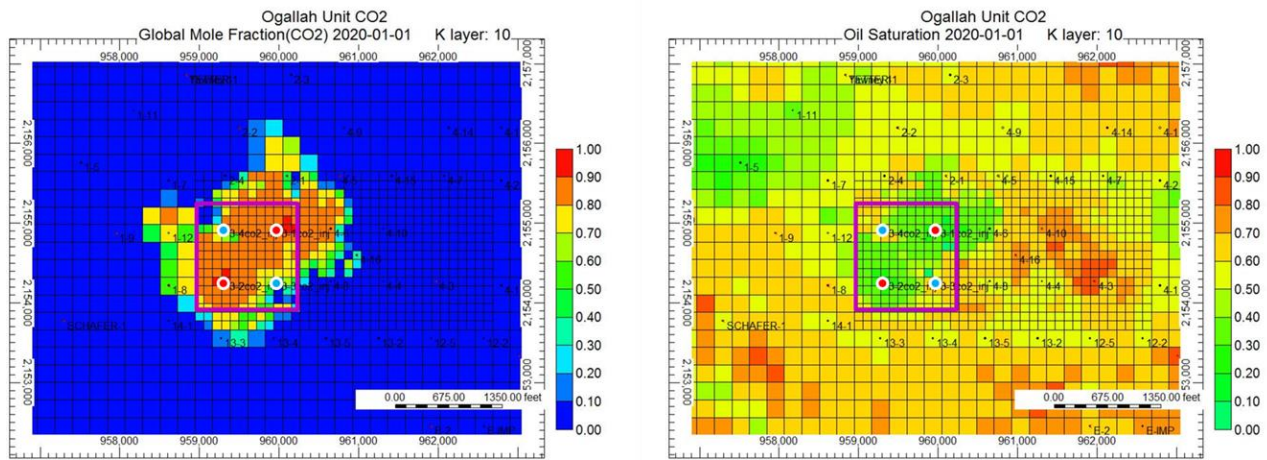
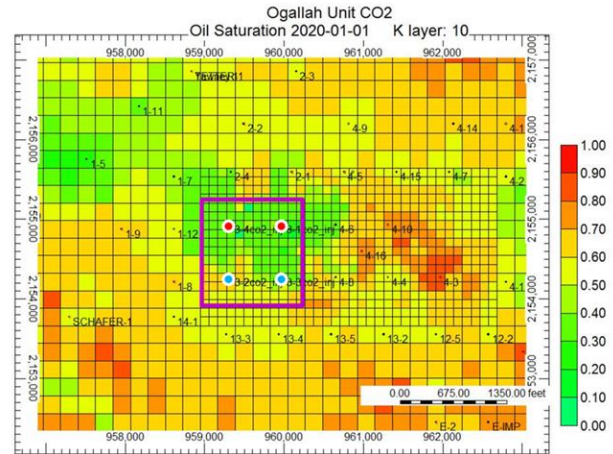
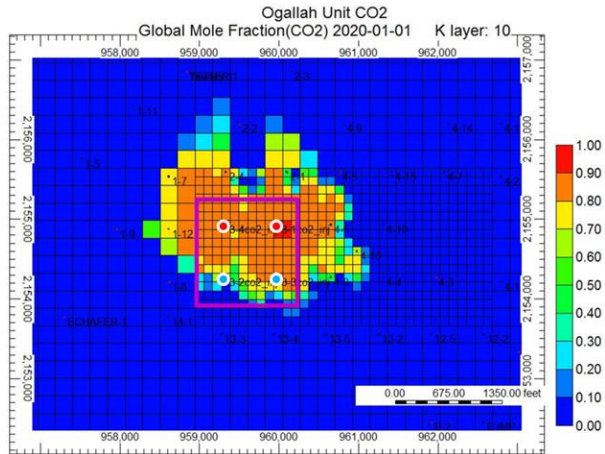
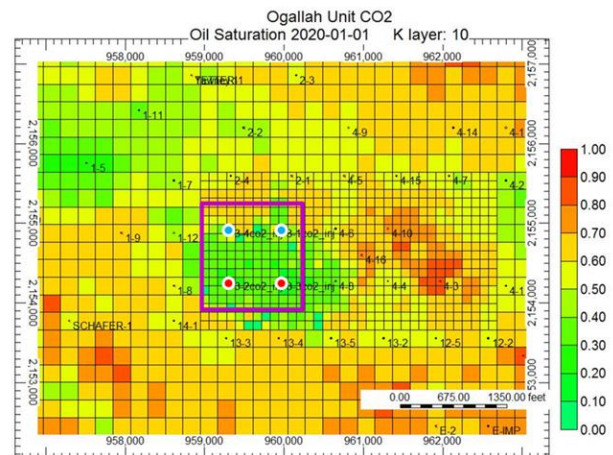
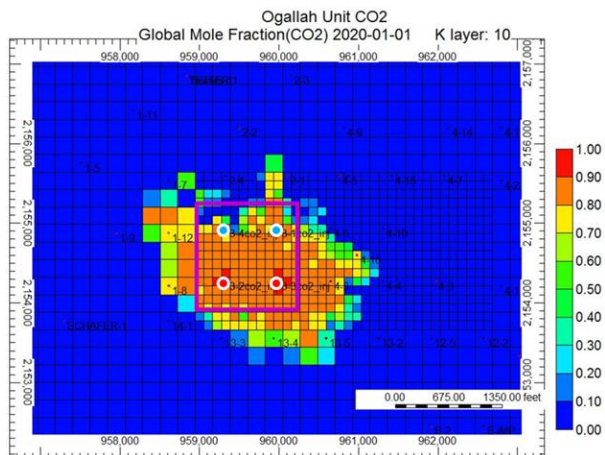


Figure 30: CO<sub>2</sub> (on the left) and oil saturation distribution (on the right) for injection pattern B, (red circles represent injectors, blue circles represent producers)



**Figure 31: CO<sub>2</sub> (on the left) and oil saturation distribution (on the right) for injection pattern C, (red circles represent injectors, blue circles represent producers)**



**Figure 32: CO<sub>2</sub> (on the left) and oil saturation distribution (on the right) for injection pattern D, (red circles represent injectors, blue circles represent producers)**

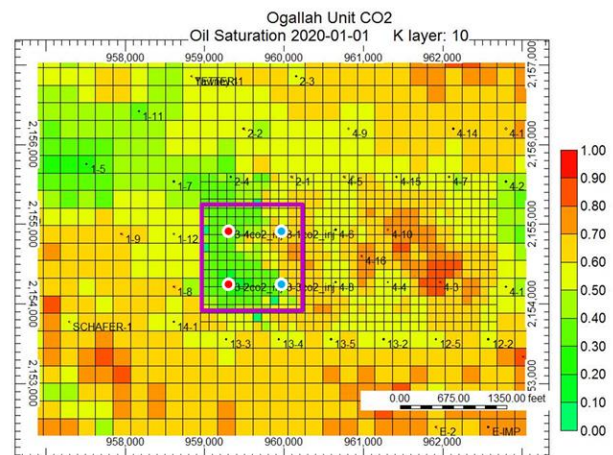
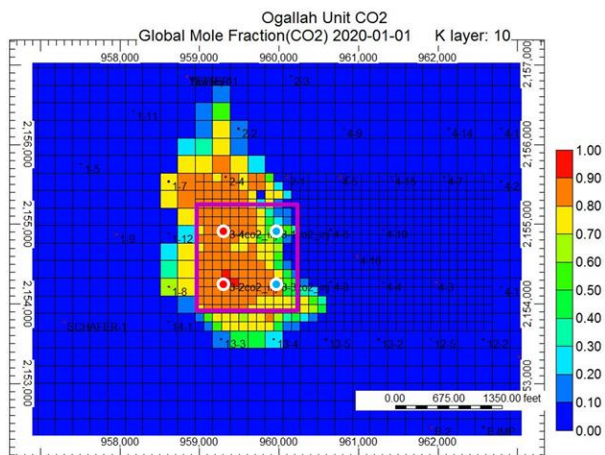


**Figure 33: CO<sub>2</sub> (on the left) and oil saturation distribution (on the right) for injection pattern E, (red circles represent injectors, blue circles represent producers)**

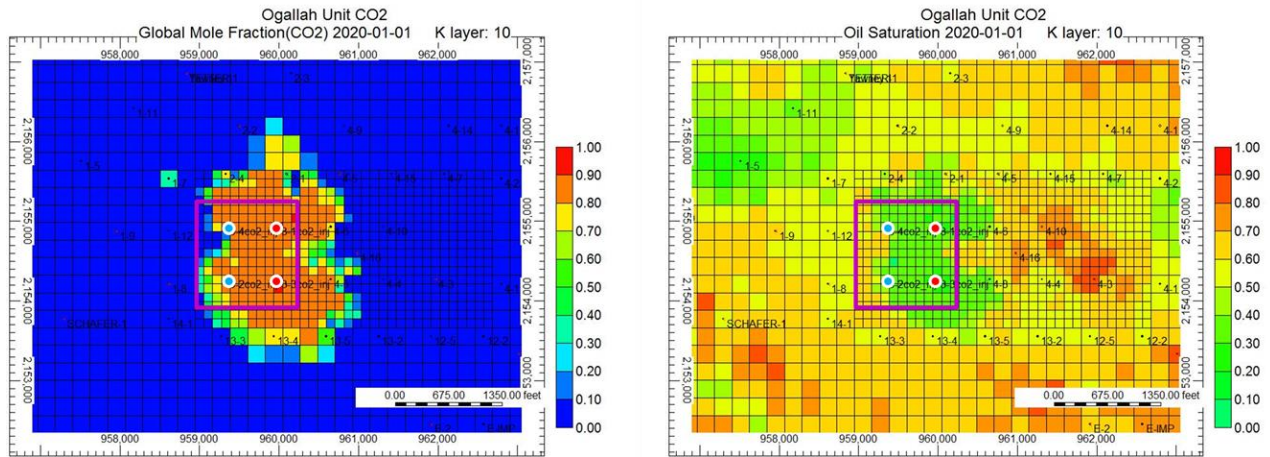


**Figure 34: CO<sub>2</sub> (on the left) and oil saturation distribution (on the right) for injection pattern F, (red circles represent injectors, blue circles represent producers)**

Table 6 summarizes the simulated production results with different pattern design. Although the incremental oil from each producer differs in each case, the same total recovered incremental oil volume is observed among various injection patterns. Injection pattern case C results in the highest incremental oil as a significant amount of oil is produced from wells in the neighboring leases. In general, the water production of the lease is reduced as a result of CO<sub>2</sub> injection. The GU of CO<sub>2</sub> varies from 61 to 79 MSCF/STB and NU of CO<sub>2</sub> varies from 57 to 75 MSCF/STB.

**Table 6: Summary of injection and production results on lease 3 with different injection pattern**

Case	A	B	C	D	E	F
CO <sub>2</sub> injected (MMSCF)	1314	1314	1314	1314	1314	1314
CO <sub>2</sub> produced (MMSCF)	95.03	10.19	11.11	14.99	5.58	57.55
CO <sub>2</sub> remained (MMSCF)	1219	1304	1303	1299	1308	1256
Incremental oil from well 3-1 (STB)	1860	0	0	2663	9164	5587
Incremental oil from well 3-2 (STB)	8911	0	10212	0	0	0
Incremental oil from well 3-3 (STB)	0	614	559	0	1607	5184
Incremental oil from well 3-4 (STB)	0	10157	0	8107	0	0
Total incremental oil from lease 3	10771	10771	10771	10770	10771	10771
Incremental oil from well 1-7 (STB)	8690	1248	8306	1137	6441	2952
Incremental oil from well 1-8 (STB)	0	3512	0	4079	0	0
Incremental oil from well 2-4 (STB)	1017	1123	1408	721	848	1442
Incremental oil from well 4-6 (STB)	0	767	770	87	0	599
Incremental oil from well 4-8 (STB)	923	299	333	884	277	905
Total incremental oil relative to Base case (STB)	21402	17718	21587	17678	18336	16669
Water production base case (MMSTB)	1.69	1.69	1.69	1.69	1.69	1.69
Water production (MMSTB)	1.28	0.37	1.27	0.39	0.03	1.60
Recovery factor	44.9	47.3	45.8	47.5	46.0	46.8
GU (MSCF/STB)	61.4	74.2	60.9	74.3	71.7	78.8
NU (MSCF/STB)	57.0	73.6	60.4	73.5	71.4	75.4

### 2.6.2 Water Alternate Gas Injection

A water alternate gas (WAG) injection process is often used to counter the tendency of quick gas breakthrough in the reservoir during CO<sub>2</sub> injection. Slugs of water are injected between slugs of gas to lower the mobility of gas behind the front and increase the sweep efficiency. It also reduces the volume of CO<sub>2</sub> that needs to be injected in the reservoir. A WAG process is explored with injection of a 0.05 PV slug of CO<sub>2</sub> alternating with a 0.05 PV slug of water in a 1:1 WAG ratio. Figure 34 shows the comparison of average pressure of lease 3 under different production conditions. The red dashed line shows the change of pressure profile during the WAG process where the pressure rises during the water injection cycle and declines during the CO<sub>2</sub> injection cycle. Although the average pressure is higher than the case when CO<sub>2</sub> is

continuously injected (red color curve), the pressure variation is generally within the pressure range of near miscible conditions. The recovery factor is improved from 44.9 to 47.7 when WAG is used in place of continuous CO<sub>2</sub> injection. The increase of average pressure in a WAG process normally would have improved the extraction mechanism, and mobility control apparently also improves the displacement efficiency under near miscible conditions.

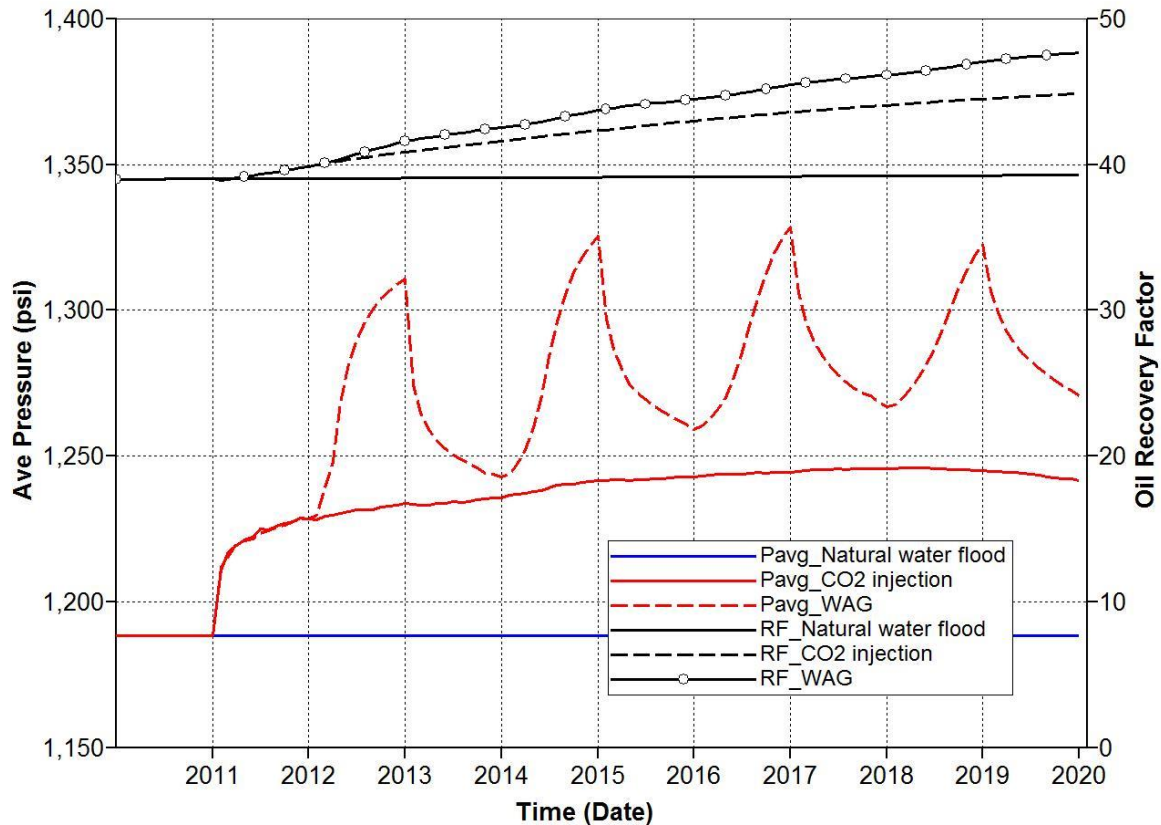


**Figure 35: Comparison of average reservoir pressure under different production conditions.**

The response of oil production to WAG on well 3-2 in case A is presented in Figure 35. The oil rate increases from 1.8 to 2.5 b/d and is sustained at that level until the end of injection. The water cut is reduced from 0.9 to 0.2 and back to 0.5 at the end of injection when GOR rises to 3100 SCF/STB. The oil production at well 1-7 in the surrounding lease also responds to the WAG process. As shown in Figure 36, the oil rate (red solid circles) rises after one cycle of WAG injection at the end of 2013 but the incremental oil production is less than that from the continuous CO<sub>2</sub> injection.

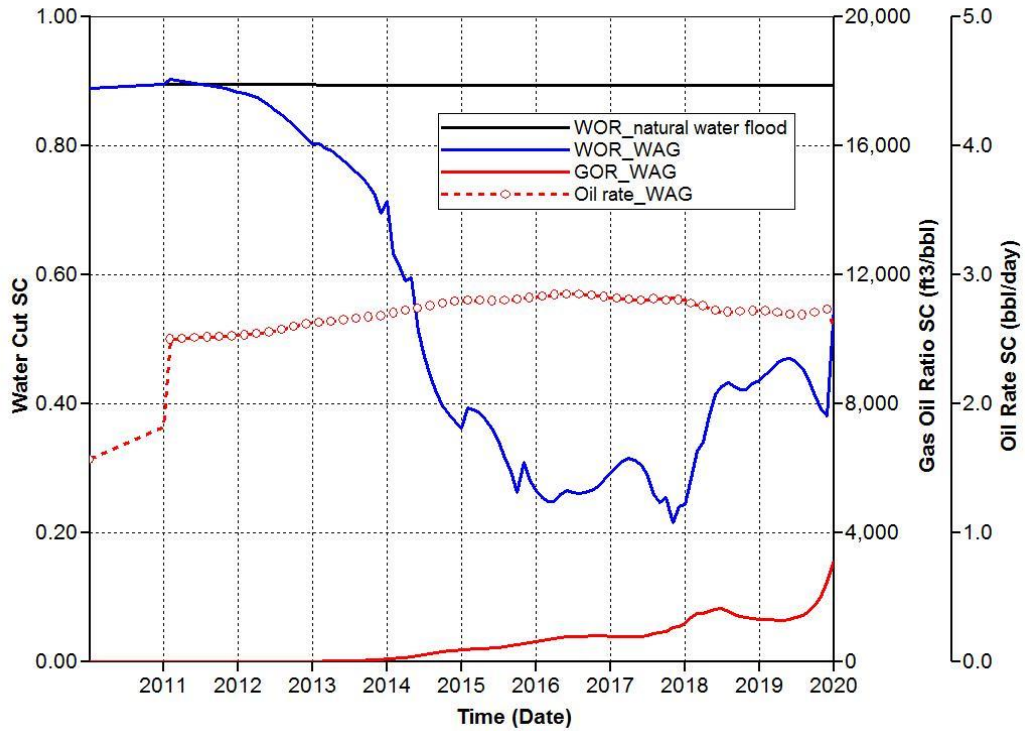


Figure 36: Production performance of well 3-2 during WAG injection.

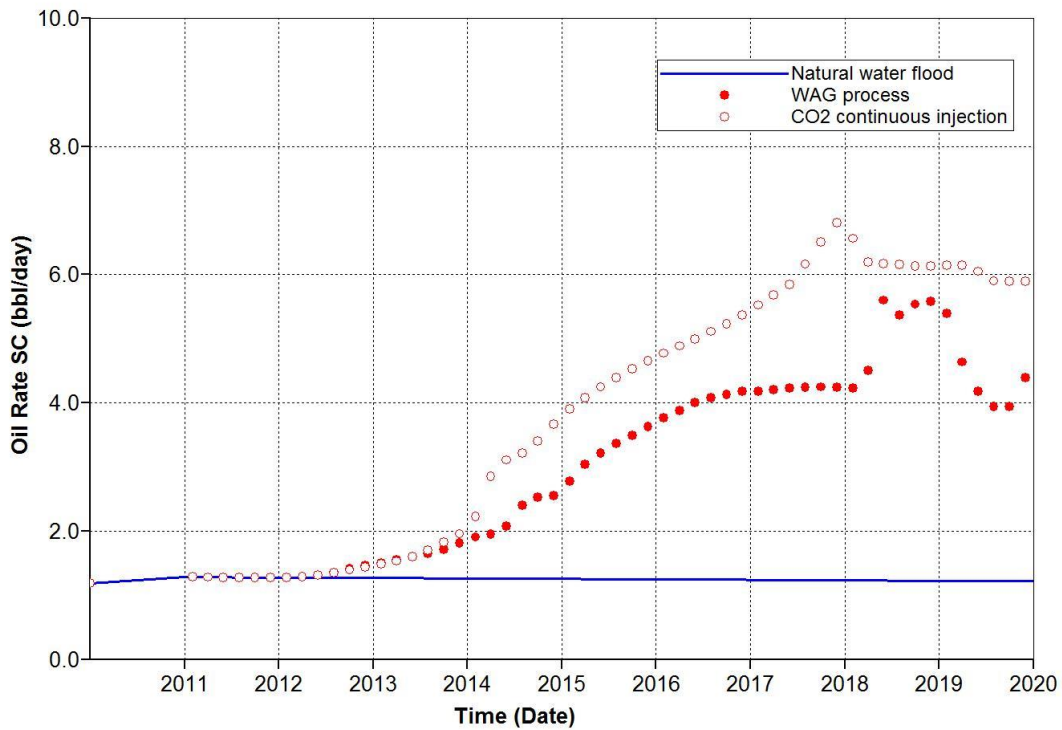


Figure 37: Oil rate responding to different injection schemes at well 1-7.

The simulation results of WAG injection in different cases are summarized in Table 7. The incremental oil recovered by the WAG process on lease 3 is similar in cases among different injection patterns. In the modeling, a small volume (0.05 PV) of CO<sub>2</sub> and water is alternately injected until 0.25 PV of CO<sub>2</sub> is injected. The comparison of total production in lease 3 between continuous CO<sub>2</sub> and WAG injection shows no difference, but the total incremental oil recovery including the neighboring wells show less recovery in the WAG process. As the water shielding and gravity segregation can affect the effectiveness of CO<sub>2</sub> in contact with unswept oil, a WAG process might result in less oil recovery than continuous CO<sub>2</sub> injection. Nevertheless, total volume of CO<sub>2</sub> injection is reduced in half. Accordingly, the GU and NU of CO<sub>2</sub> are significantly reduced and varied from 37 to 50 MSCF/STB.

**Table 7: Summary of WAG process on lease 3 with different injection pattern**

Case	A	B	C	D	E	F
CO <sub>2</sub> injected (MMSCF)	730	730	730	730	730	730
CO <sub>2</sub> produced (MMSCF)	19.0	6.73	1.59	5.45	2.11	16.9
CO <sub>2</sub> remained (MMSCF)	711	723	728	725	728	713
Incremental oil from well 3-1 (STB)	1862			4165	9213	7101
Incremental oil from well 3-2 (STB)	8908		10256			
Incremental oil from well 3-3 (STB)		667	515		1558	3669
Incremental oil from well 3-4 (STB)		10104		6606		
Total incremental oil from lease 3	10770	10771	10771	10771	10771	10770
Incremental oil from well 1-7 (STB)	5913	906	6305	304	4275	2903
Incremental oil from well 1-8 (STB)	0	1610	0	1594	0	0
Incremental oil from well 2-4 (STB)	1086	1306	1575	677	903	1241
Incremental oil from well 4-6 (STB)	0	409	562	3	0	360
Incremental oil from well 4-8 (STB)	895	364	337	1085	360	721
Total incremental oil relative to Base case (STB)	18664	15365	19550	14433	16308	15996
Water production base case (MMSTB)	1.69	1.69	1.69	1.69	1.69	1.69
Water production (MMSTB)	1.28	0.37	1.27	0.39	0.03	1.61
Recovery factor	47.7	50.9	48.0	51.2	48.8	49.5
GU (MSCF/STB)	39.1	47.5	37.3	50.6	44.8	45.6
NU (MSCF/STB)	38.1	47.1	37.3	50.2	44.6	44.6

## Summary

1. A new geological model was developed based on an integrated methodology in generating the porosity–permeability profile and rock types at well locations where no core data was available. Sequential Gaussian Simulation was used to populate porosity and permeability in the final geological model which captures the characteristics of geological trends and retain reservoir heterogeneities
2. The primary production history of a 47 acre lease (lease 3) containing four wells was reasonably matched. This lease was examined for a near miscible CO<sub>2</sub> injection process with different patterns and injection schemes.
3. The simulation results indicate that near miscible displacement is achievable in the lease at current reservoir operation pressure. The simulated displacement efficiency in the lease was improved on average from 39% to 46% with continuous CO<sub>2</sub> injection and to 49% with a WAG process.
4. The gross utilization and net utilization of CO<sub>2</sub> calculated from the model are higher than those most commonly observed in miscible flooding applications.

### 3. SINGLE WELL PILOT TEST

The second part of this report describes an actual field pilot test conducted in a well producing from the Arbuckle formation to demonstrate the feasibility of using CO<sub>2</sub> injection at near miscible conditions to mobilize the oil. (Tsau, et al., 2014) More than seven oil fields producing from Arbuckle reservoirs were considered for the pilot test. The final pilot test was conducted on Dreiling #10 in the Dreiling field, Ellis County, Kansas. The reservoir temperature was 106 °F and the well shut-in pressure was 1150 psi. The minimum miscibility pressure (MMP) determined in the lab was 1500 psi at reservoir temperature. The single well pilot test was designed to experimentally inject CO<sub>2</sub> into the Arbuckle formation at pressures below MMP to determine the efficiency of CO<sub>2</sub> displacement at near miscible conditions. The pilot test consists of two chemical tracer tests with one CO<sub>2</sub> injection in between. The first chemical tracer test was performed to determine the oil saturation in the formation prior to CO<sub>2</sub> injection. This was followed by injecting approximately 17 tons of CO<sub>2</sub> at pressures below MMP with a follow-up water displacement to move mobilized oil and CO<sub>2</sub> from the area of investigation, followed by a second tracer test performed to determine the remaining oil saturation.

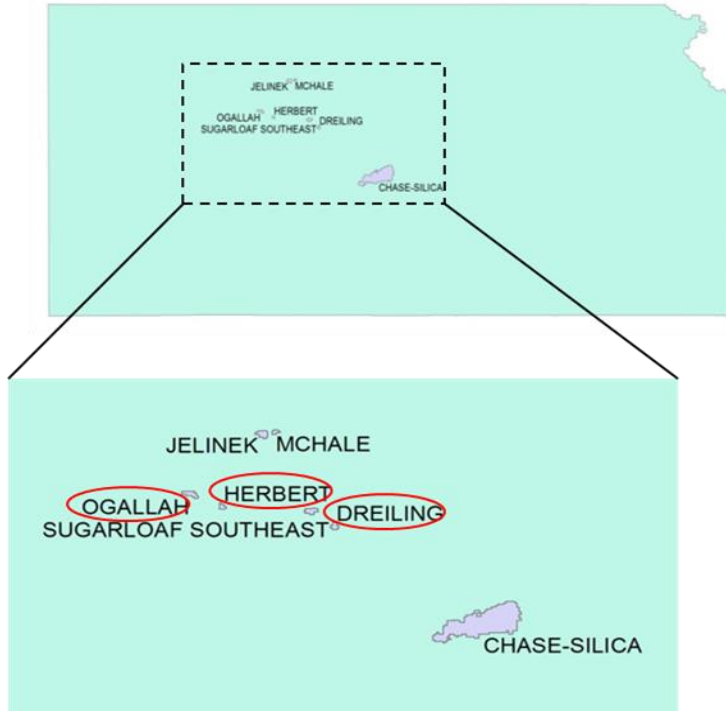
#### 3.1 Candidate Well Selection

Several oil fields producing from Arbuckle reservoirs were considered in selection of the well for the proposed single well pilot test. Table 8 summarized the location of the oil fields, reservoir temperature, and pressure surveyed at the time of consideration. Figure 37 shows the location of these oil fields, which are relatively close to the Ogallah unit at Trego County. The Arbuckle formation in these oil fields is associated with structural highs on the Central Kansas uplift (Franseen, et al., 2004).

**Table 8: Oil fields considered for single well pilot test**

Field	County	Reservoir Temperature (F)	Reservoir pressure (psi)
Jelinek	Rooks	88-120	906-1060
McHale	Rooks	92-112	926-1057
Sugarloaf Southeast	Ellis	100-121	987-1071
Herbert	Trego	98-125	1000-1127
Chase-Silica	Barton	110-113	915
Dreiling	Ellis	106	1145

The parameters used in screening the candidate well for single well pilot tests include the depth of well, reservoir temperature, current reservoir pressure, and MMP at reservoir conditions. Among all the wells prescreened, three wells were selected for further evaluation.



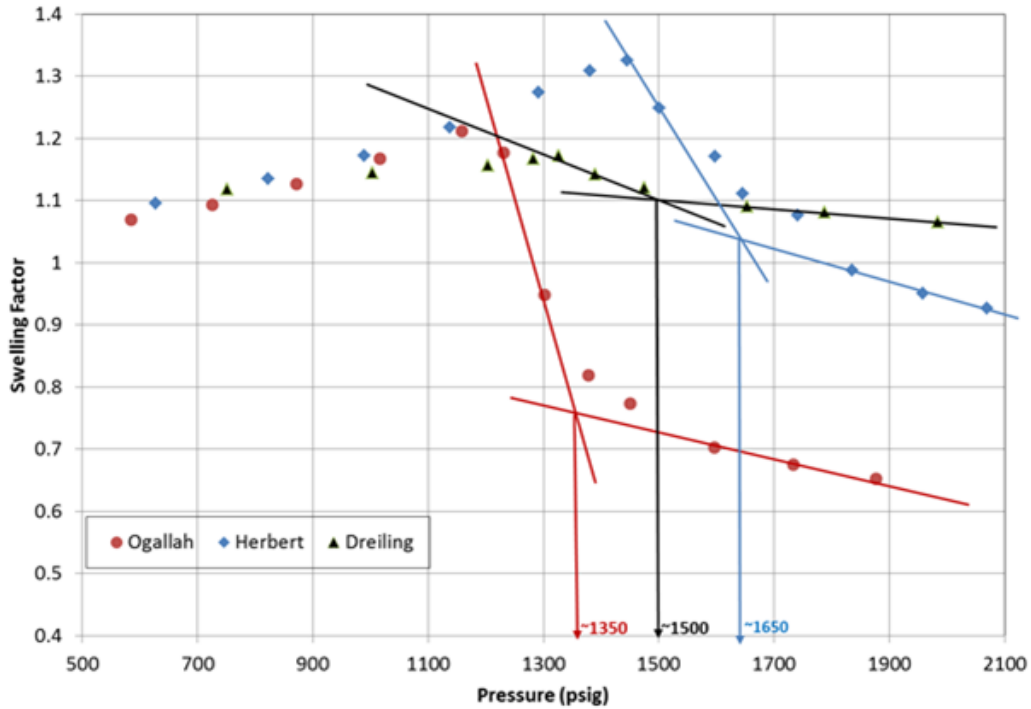
**Figure 38: Locations of selected oil fields in state of Kansas.**

Table 9 summarizes selected parameters and other relevant properties of oil from these three wells. The MMP reported for the Ogallah well was derived from an in-house developed swelling/extraction test and confirmed by slim-tube experiment (Tsau et al., 2010). The rest of the MMPs were derived from swelling tests. Figure 38 presents the swelling test results of these oil samples and the MMP estimation. The MMP of the sample oil is determined graphically based on the intersection of lines drawn in each set of test results.

**Table 9: Candidate well list**

Well #	1	2	3
Field	Ogallah	Herbert	Dreiling
Well depth (ft)	4000	3902	3450
Reservoir temp (°F)	110	125	106
Reservoir pressure (psia)	1200	1127	1145
API gravity	33.3	37.6	30.6
Molecular weight of Oil (g/mole)	228.7	212.5	255.5
Viscosity (cp) @ reservoir temp	4.5	10.0	10.5
MMP (psia)	1350	1650	1500

The third well in Table 9 in the Dreiling field was selected for the single well pilot test because its reservoir conditions meet the near miscible conditions (the pressure was within 75-80% of MMP) as defined in our previous study and the well provided by Downing Nelson Company Inc. was available for a field test.



**Figure 39: MMPs determined with a swelling/extraction test on sample oil from candidate well.**

Figure 39 shows the neutron density log with part of the well configuration near perforation depth. It shows three zones opened in the Arbuckle formation at depths of 3413-3416', 3422-3425' and 3437-3440' (yellow colored zones) with an average porosity reading of 12%, 8%, and 10% (red color line) respectively.

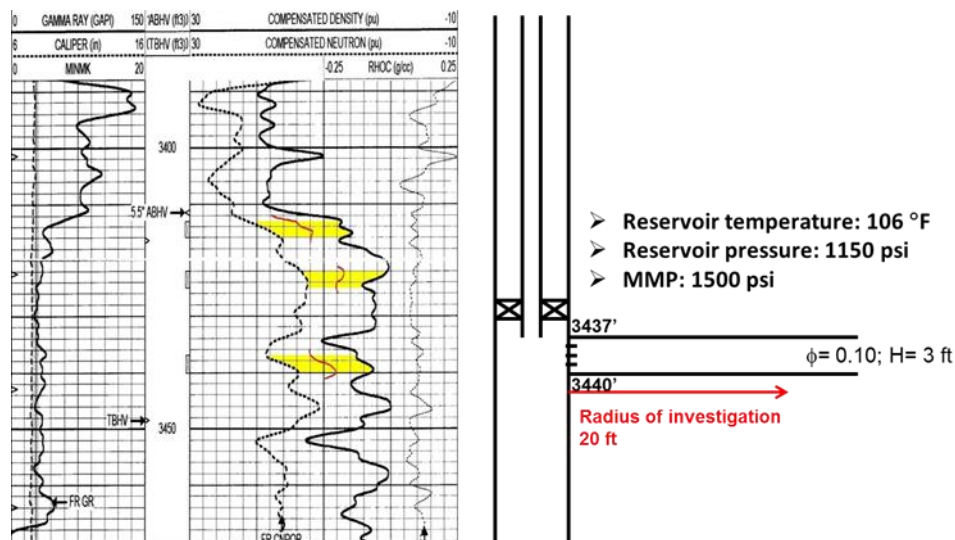


**Figure 40: Neutron density log with well configuration of candidate well for the pilot test.**

The bottommost perforation interval was selected as the target zone for the test as it is convenient for injecting fluid into this zone with a packer set at 2 feet above the zone's perforations to isolate the other zones. The well contains 2-3/8" tubing and was produced via rod pump at about 200 bpd of fluids with 0.33% oil cut prior to commencement of the pilot test.

### 3.2 Field Operation

The pilot test consists of a single-well chemical tracer test before and after CO<sub>2</sub> injection. The first chemical tracer test was performed to determine the oil saturation in the formation prior to CO<sub>2</sub> injection. This was followed by injecting CO<sub>2</sub> at pressures below the MMP with a follow-up water displacement, followed by a second tracer test to determine the remaining oil saturation. The effectiveness of near miscible CO<sub>2</sub> displacement was determined by the reduction of oil saturation within the radius of investigation around the wellbore. The test size for a 20 feet radius of investigation corresponds to approximately 67 bbl of pore volume with an average porosity of 10% and layer thickness of 3 feet.

Chemical Tracers, Inc (CTI) was contracted to perform both single-well chemical tracer tests and Praxair was contracted to perform the CO<sub>2</sub> injection.

In the single well tracer test, a solution of primary chemical tracer (ethyl formate) is pumped downhole with material balance tracer (methanol) and cover tracer (propyl alcohol), displaced with brine, shut-in to allow hydrolysis of a portion of the ester to ethanol, which becomes a secondary non-partitioning tracer, then produced back. Since ethyl formate partitions into the oil phase and the other tracers, including the produced ethanol, do not, the ethyl formate

will arrive back at the producer later (Deans and Carlisle, 2007). The amount of separation between ethyl formate and ethanol depends on the amount of oil present in the pore space and the ester partition coefficient  $K$  that is equal to the ratio of concentration of ester in oil to that in water at equilibrium conditions. With measurement of the separation in producing profiles of ethanol and unreacted ester, or the retardation factor  $\beta$  in terms of retardation time between the arrival of two tracers in the field, the residual oil saturation  $S_{or}$  can be estimated by  $S_{or} = \beta / (\beta + K)$ . Figure 40 is a schematic representation of typical tracer profiles during backflow for estimation of residual oil saturation in the investigated zone.

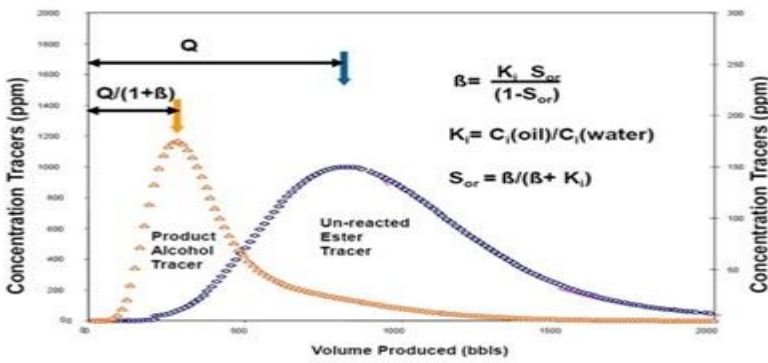


**Figure 41: Schematic representation of typical tracer profiles during backflow for interpretation.**

The  $K$ -value was measured at CTI's laboratory with synthesized reservoir brine and the sampled crude oil at the reservoir temperature. Table 10 summarizes the  $K$  values measured with brine of 66,000 ppm TDS and reservoir crude oil at reservoir temperature of 106 °F. The  $K$  value varies from 1.97 to 2.08 in the range of ester concentrations from 2,213 ppm to 9,279 ppm. The  $K$  value of 2.0 was used in calculation of residual oil saturation with  $\beta$  factor measured from the field test, in which the accuracy of  $S_{or}$  calculation is merely affected by  $K$  value within 4% of uncertainty.

**Table 10: Partition coefficient  $K$  value measurement**

Ethyl Formate Concentration (ppm)	$K$ -value
2213	2.08
3938	1.97
5210	2.01
6984	2.05
8023	2.04
9216	1.98
9279	2.06

### 3.2.1 First Tracer Test

Prior to the first chemical tracer test, the well was first treated with 150 gallons of 15% hydrochloric acid to improve injectivity. Then 150 bbl of produced water was injected to ensure the injectivity was checked and test zone was flushed to residual. A small push-pull test followed to ensure the well showed a good flow conformance with 35 bbls of 1100 ppm methyl-alcohol injected (push) and 74 bbls of back production (pull). Subsequently, 20 bbls of injected fluid containing 10,300 ppm partitioning tracer, ethyl formate (EtF), and non-partitioning tracer, (5,300 ppm n-propyl alcohol, 1,700 ppm methyl alcohol) were injected at a rate of 300 bpd with a sub-ambient wellhead pressure. Following the initial bank were 89 bbls of injected water containing 1,700 ppm Methyl alcohol at 340 bpd with sub-ambient wellhead pressure. The well then was shut-in for 2 days to allow hydrolysis of EtF, which results in formation of Ethanol (EtOH) upon reacting with formation water. The well then was produced back for a total of 200 bbls over a 1.35 day period. Samples of the produced fluid were taken every 15 min to 30 min and tracer content was analyzed by gas chromatography on-site immediately. Table 11 summarizes the first tracer test design from the injection to shut-in and into the production period.

**Table 11: Design of first chemical tracer test**

Injection Period				
Injection bank	Ethyl Formate (ppm)	n-Propyl alcohol (ppm)	Methyl alcohol (ppm)	Volume injected (bbl)
Ester	10,300	5300	1700	20
Push			1700	89.5
Shut –in period				
2.0 days				
Production period				
1.35 day; 200 bbls				

### 3.2.2 CO<sub>2</sub> Injection

After completion of the first tracer test, the well was kept producing at 200 bbl/day until the CO<sub>2</sub> injection equipment could be rigged up at the site. CO<sub>2</sub> was injected at an average rate of 535 bpd for 6.25 hours. During the injection of CO<sub>2</sub>, the bottomhole pressure and temperature were measured with a downhole gauge. Figure 41 presents the history of bottomhole pressure, temperature, injection rate and cumulative injection volume during the injection. The bottomhole

pressure was well maintained below MMP, 1500 psi, and temperature was maintained approximately at 103 °F, which assures that the displacement of CO<sub>2</sub> in the formation is maintained at near miscible conditions. The total amount of CO<sub>2</sub> injected at reservoir conditions is about 140 bbl, which represents 2 PV of volume investigated in the radius of 20 ft around the wellbore.

Approximately 17 tons of CO<sub>2</sub> was injected at near miscible conditions to displace the oil remaining in the radius of investigation. Following the CO<sub>2</sub> injection, an additional 1,600 bbl water was injected to displace any mobilized oil outside the 20 foot of investigation radius and to dissolve the trapped CO<sub>2</sub> in the pore space in preparation for the second chemical tracer test.

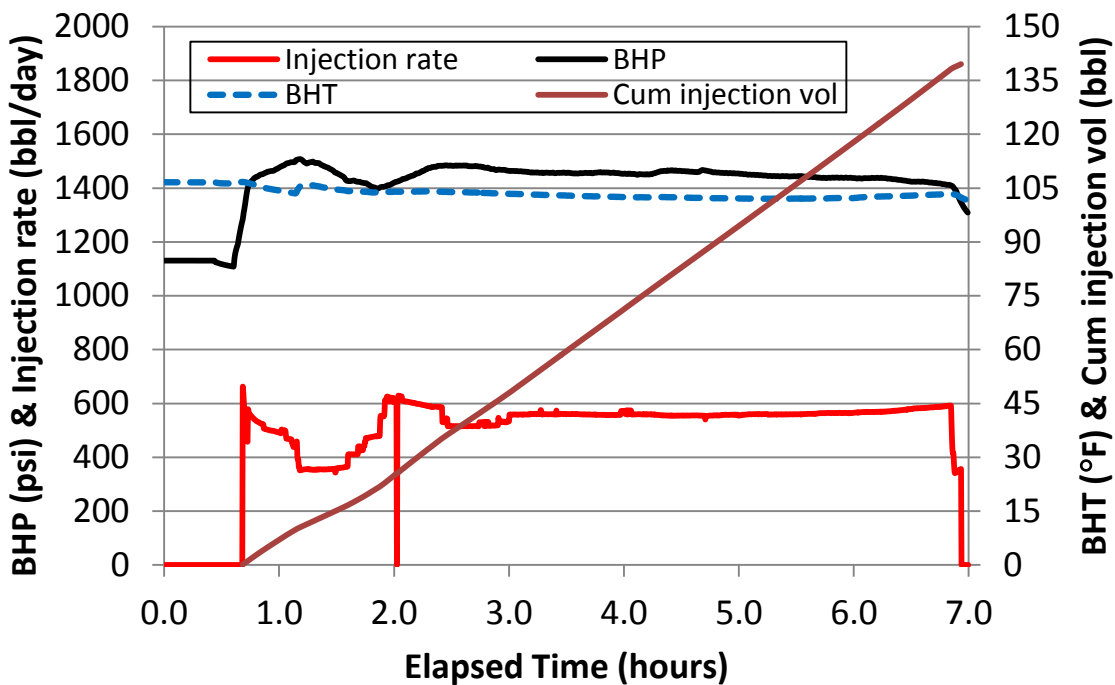


Figure 42: CO<sub>2</sub> injection history with downhole pressure and temperature measurements.

### 3.2.3 Second Tracer Test

The second single well tracer test was conducted in a similar way as the first. Table 12 summarizes the second test design. The ester bank, 20 bbls of 66,000 ppm TDS water containing 9,700 ppm EtF, 4,900 ppm n-Propyl alcohol and 2,200 ppm MeOH was injected at 300 bpd with a sub-ambient wellhead pressure. The push bank, 89.5 bbls of 66,000 ppm TDS

water containing 2,200 ppm MeOH was injected at a rate of 450 bpd with a 450 psi wellhead pressure. The well was shut-in for 2.4 days to allow ethyl formate to hydrolyze to form ethanol. The well was produced back for a total of 197 bbls of water production over a one day period. Samples of the production fluid were taken by CTI every 15 to 30 min and analyzed for tracer content by gas chromatography on-site.

**Table 12: Design of second chemical tracer test**

Injection Period				
Injection bank	Ethyl Formate (ppm)	n-Propyl alcohol (ppm)	Methyl alcohol (ppm)	Volume injected (bbl)
Ester	9700	4900	2200	20
Push			2200	89.5
Shut –in period				
2.4 days				
Production period				
1.03 day; 197 bbls				

An ideal tracer test assumes that tracer injected into a homogeneous layer will follow the streamlines that extend radially from the wellbore into the test formation. The produced ethanol from the hydrolysis of ester during the well shut-in period and unreacted ester will also return radially along the same streamlines to the well during the production. But in most cases the tracer profiles obtained in the field display some non-ideal behaviors affected by fluid drift, flow irreversibility, cross-flow between layers and complexity in pore systems (Deans and Carlisle, 1986). To account for these non-idealities and complexity of carbonate reservoirs, a proprietary simulator, CFSIM by Chemical Tracers Inc., was applied to match the field data and determine the  $\beta$  factor and thus the residual oil saturation. This model allows the simulation to replicate various features of the tracer data by adjusting parameters to account for different tracer profile characteristics and determine the  $\beta$  factor more accurately than relying on graphical determination from the apex of both the ethanol and ester profiles.

Figure 42 presents the produced profiles of ethanol (EtOH) and unreacted tracer ethyl formate (EtF) during the first tracer test. The red triangles represent field data of EtOH whereas blue squares represent unreacted EtF. The solid lines represent the model match results. From the graph, the x-axis separation of the two tracer curves indicates how much slower the unreacted ester tracer returned to the well than the product ethanol. The  $\beta$  factor derived from this test is 0.597 and the residual oil saturation is estimated to be 0.23 with K value of 2.0.

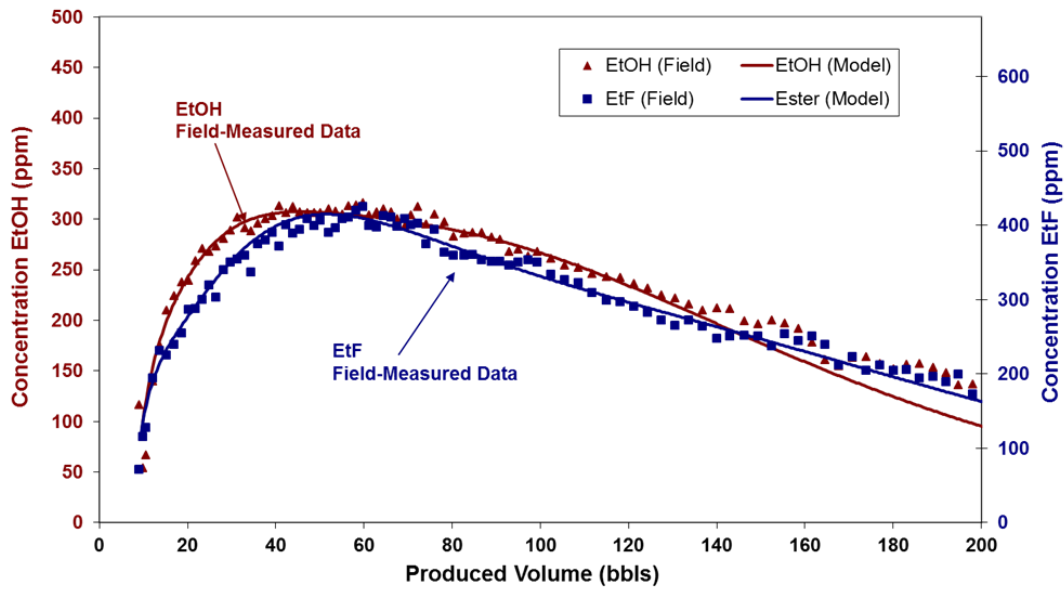


**Figure 43: Produced tracer profiles from the first chemical tracer test.**

Figure 43 presents the results from the second tracer test. The red triangles represent field data of EtOH whereas blue squares represent unreacted EtF. The solid lines represent the model matched results. The  $\beta$  factor derived from this test is 0.50 and the residual oil saturation is 0.20.

The oil saturation measured from the two tracer tests were 0.23 and 0.20, respectively. A reduction of oil saturation by 0.03 represents a 13% improvement of oil displacement, which results from CO<sub>2</sub> injection at near miscible conditions. To our knowledge, this is the first set of measured residual oil saturations in the Arbuckle formation available in the public domain. To demonstrate the efficiency of CO<sub>2</sub> EOR at near miscible conditions more tests conducted in other oil fields are needed.

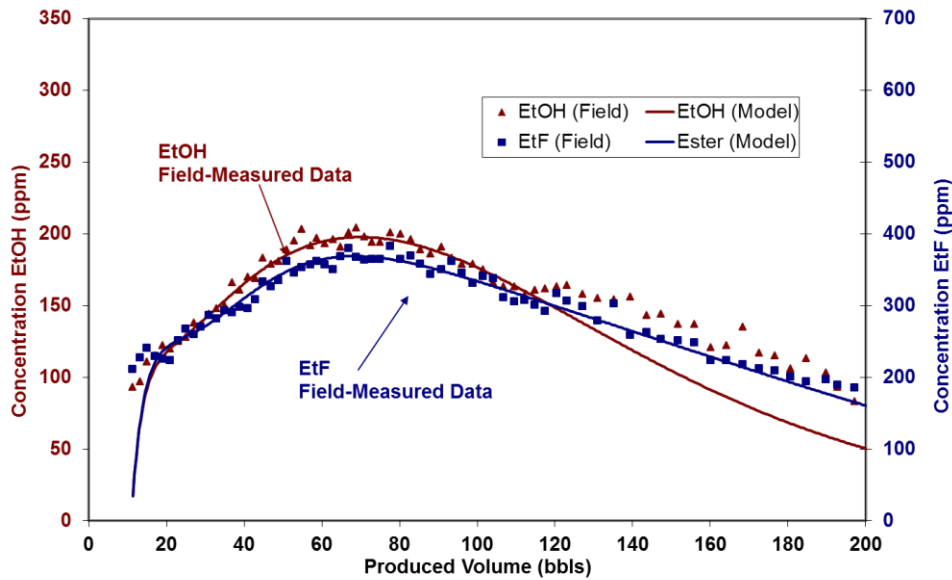
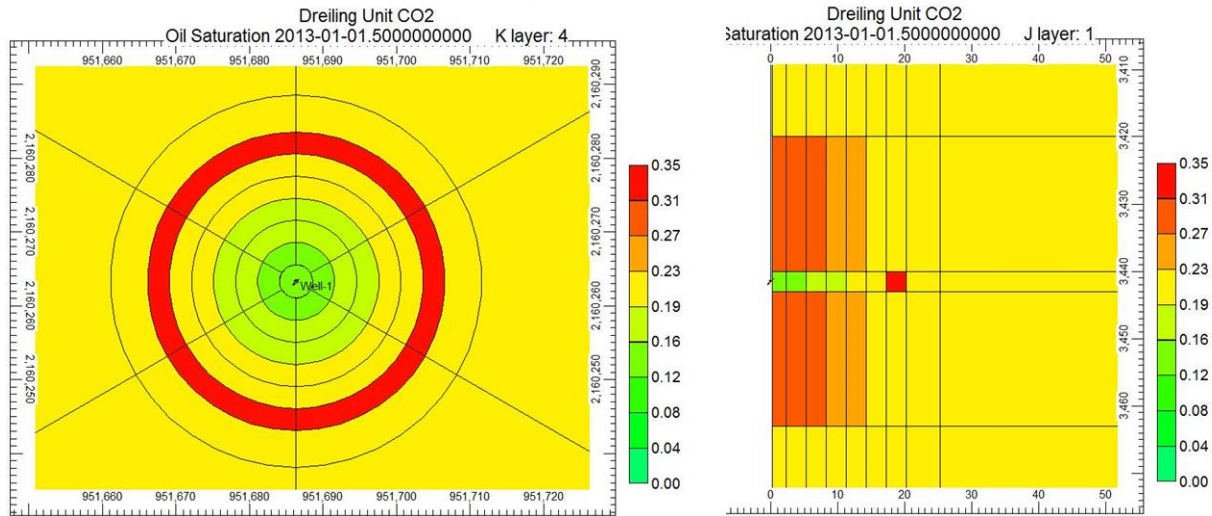


Figure 44: Production tracer profile from the second tracer test after CO<sub>2</sub> injection.

### 3.3 Computation Modeling

A simplified well model created with CMG's GEM (2010) was alternatively used to simulate a process of CO<sub>2</sub> injection and evaluate the uncertainty of residual oil saturation responding to the CO<sub>2</sub> displacement at near miscible conditions. The radial well model consists of 8 layers in the vertical direction and 10 grids in the radial direction. A bottom drive aquifer was included in the model to provide pressure support from the bottommost layer. Presented in Figure 44 is the simulated oil distribution around the target well at stages of CO<sub>2</sub> injection. The oil bank with higher saturation was formed in the target zone (3 ft thin layer in the model) during the CO<sub>2</sub> injection. Figure 45 shows the simulated oil distribution around the target well after CO<sub>2</sub> injection followed by water injection. The oil bank formed in the target zone was pushed away further from the wellbore indicating the oil was mobilized by CO<sub>2</sub> and displaced by water in the model.



**Figure 45: Simulated oil saturation distribution at the end of CO<sub>2</sub> injection. (areal view on the left and cross-section on the right)**

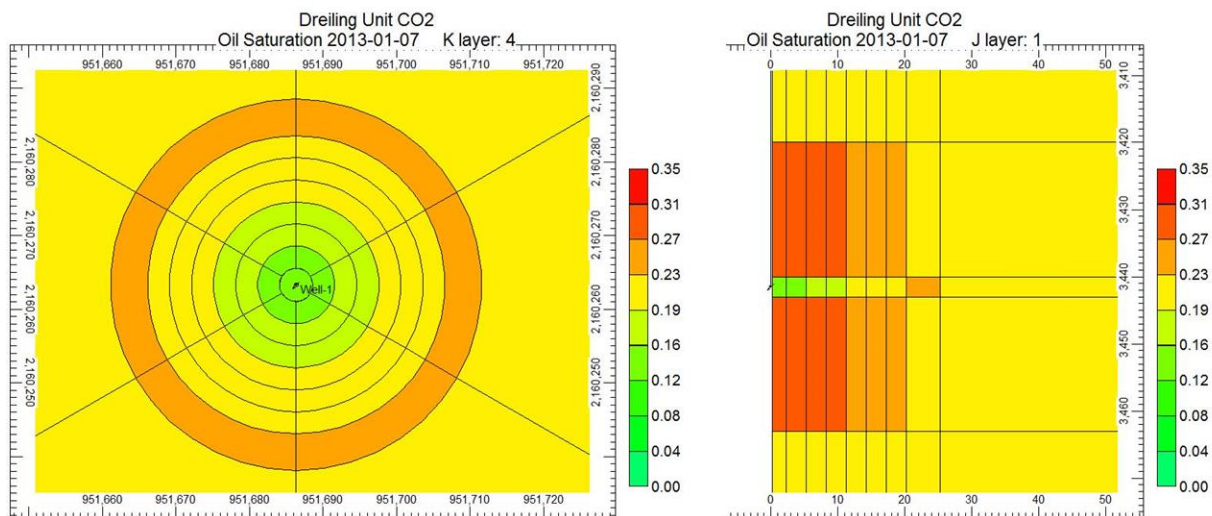


**Figure 46: Simulated oil saturation distribution at the end of water injection. (areal view on the left and cross-section on the right)**

During the simulated CO<sub>2</sub> injection, the injection pressure was controlled at below the 1,500 psi MMP at reservoir temperature. Figure 46 shows the pressure distribution in the simulation for grid blocks around the wellbore during the fluid injection. The pressure rises from 1,150 psi to 1,500 psi at the very beginning of CO<sub>2</sub> injection and declines later, then rises again due to the water injection. Although the pressure varies in the region of investigation, it was well maintained in the near miscible envelope at pressures between MMP and 0.8 MMP. A similar trend is also observed with CO<sub>2</sub> injection increased from 2 PV to 4 PV (Figure 47)

wherein the pressures within the region of 20 ft are all maintained under near miscible conditions.

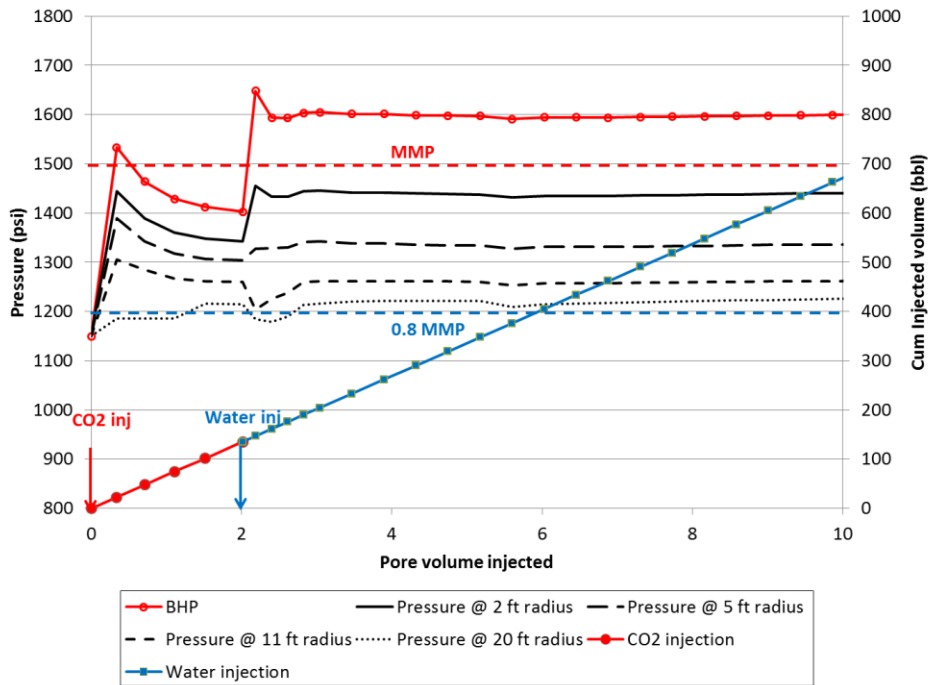


Figure 47: Pressure distribution from the simulation calculation indicating the pressure inside the radius of investigation (20 ft) is maintained at near miscible conditions with 2 PV CO<sub>2</sub> injection.

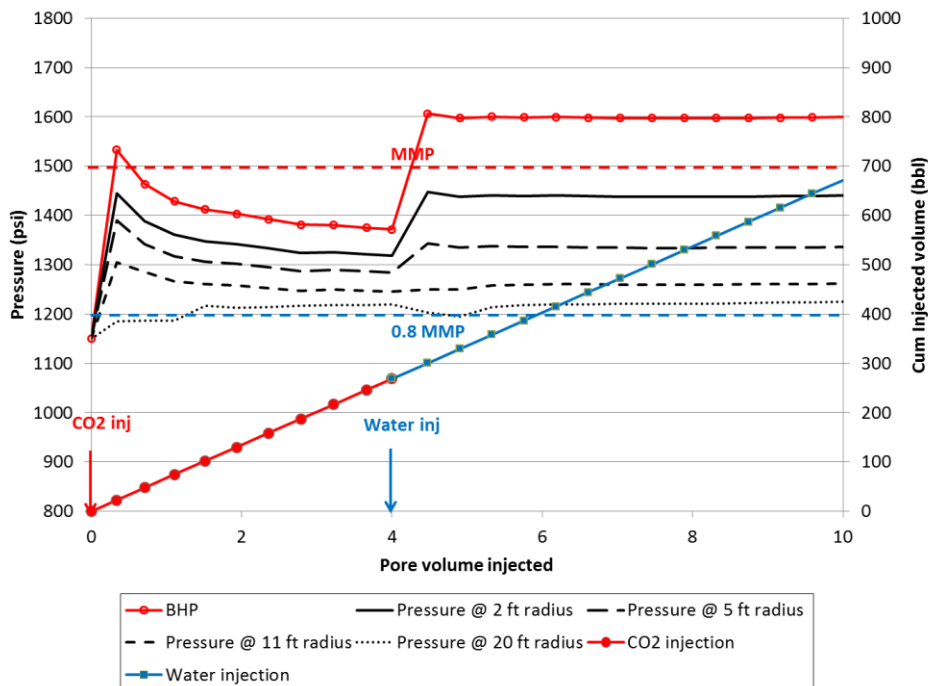


Figure 48: Pressure distribution from the simulation calculation indicating the pressure inside the radius of investigation (20 ft) is maintained at near miscible conditions with 4 PV CO<sub>2</sub> injection.

Table 13 summarizes the oil saturation change in the model due to the displacement of CO<sub>2</sub> as described. The simulation demonstrates that if the oil saturation were 0.23 as measured in the first tracer test, then the remaining oil saturation in the region of investigation after CO<sub>2</sub> and water injection is 0.192, very close to that measured from the second tracer test.

**Table 13: Residual oil saturation calculated from the simulation**

Sorw	0.3	0.25	0.23	0.2
Sorco2	0.252	0.210	0.192	0.168

To examine the effect of CO<sub>2</sub> injected volume on the displacement efficiency, the same model was used with CO<sub>2</sub> injection volume increased from 2 to 4 PV and the pressure near the wellbore being controlled between the MMP and 0.8 MMP as shown in Figure 42., An improvement of efficiency is observed with the increased CO<sub>2</sub> injection. Table 14 presents the change of oil saturation in the region of investigation under the different scenarios. The displacement efficiency is increased with the CO<sub>2</sub> injected volume. At a higher CO<sub>2</sub> injection volume, better displacement efficiency is also observed at higher waterflood residual oil saturation prior to CO<sub>2</sub> injection.

**Table 14: Effect of CO<sub>2</sub> injected volume on displacement efficiency at near miscible conditions**

Sorw	Sorco2 after CO <sub>2</sub> injection of		% change	
	2.0 PV	4.0 PV	2.0 PV	4.0 PV
0.3	0.252	0.233	16.00	22.33
0.25	0.210	0.201	16.00	19.60
0.23	0.192	0.186	16.52	19.13
0.2	0.168	0.163	16.00	18.50

### Summary

The single well pilot test and simple model calculation demonstrate the potential of using CO<sub>2</sub> injection at near miscible conditions to improve oil recovery in Kansas Arbuckle reservoirs and others where MMP cannot be achieved. Some findings drawn from this work are:

1. The residual oil saturation in the tested Arbuckle formation with natural water flooding prior to CO<sub>2</sub> injection was 0.23. The residual oil saturation in the same tested zone after CO<sub>2</sub>

injection at near miscible conditions was 0.20. The three units of oil saturation reduction represent a 13% improvement of oil displacement in a tertiary oil recovery process.

2. Single well chemical tracer tests were successfully applied to determine residual oil saturation in a carbonate formation subjected to natural water flooding and CO<sub>2</sub> injection.
3. A simplified radial well model is applicable to demonstrate the process of using CO<sub>2</sub> injection at near miscible conditions to improve displacement efficiency.

#### 4. SUMMARY AND CONCLUSIONS

This project describes a research program to demonstrate the application of CO<sub>2</sub> displacement at near miscible pressure for improved oil recovery. The results are presented in two parts: 1) computational simulation study and 2) single well pilot test. The computational study discusses the methodologies of developing a geological model and assessment of oil recovery from CO<sub>2</sub> injection at near miscible conditions by reservoir simulations. The single well pilot test discusses the implementation of the single well chemical tracer test prior to and after CO<sub>2</sub> injection in determination of the residual oil saturation to quantify the effectiveness of the CO<sub>2</sub> displacement process at near miscible conditions. Some of the conclusions drawn from this research are summarized as follows:

1. A new geological model was developed based on an integrated methodology in generating porosity-permeability profiles and rock types at well locations where no core data was available. Sequential Gaussian Simulation was used to populate porosity and permeability in the final geological model which captures the characteristics of geological trends and retain reservoir heterogeneities
2. The primary production history of a 47 acre lease (Ogallah lease 3) containing four wells was reasonably matched. This lease was examined for a near miscible CO<sub>2</sub> injection process with different patterns and injection schemes.
3. The simulation results indicate that near miscible displacement is achievable on the lease at current reservoir operation pressure. The displacement efficiency on the lease was improved on average from 39% to 46% with continuous CO<sub>2</sub> injection and to 49% with a WAG process.
4. The gross utilization and net utilization of CO<sub>2</sub> calculated from the model are higher than those most commonly observed in miscible flooding applications.
5. The residual oil saturation in the tested Arbuckle formation with natural water flooding prior to CO<sub>2</sub> injection was 0.23. The residual oil saturation in the same tested zone after CO<sub>2</sub> injection at near miscible conditions was 0.20. The three units of oil saturation reduction represent a 13% improvement of oil displacement in a tertiary oil recovery process.
6. Single well chemical tracer tests were successfully applied to determine residual oil saturation in a carbonate formation subjected to natural water flooding and CO<sub>2</sub> injection.

7. A simplified radial well model is applicable to demonstrate the process of using CO<sub>2</sub> injection at near miscible condition to improve displacement efficiency.

## **5. TECHNOLOGY TRANSFER**

During the course of this project, the research team has given presentations at various events sponsored by RPSEA and SPE, and oil and gas industry. Two papers were published and nine presentations were given. Notable accomplishments in this project include: 1) developed an integrated method to predict porosity and permeability from microresistivity logs, 2) constructed a reservoir model of Ogallah unit with limited data for a mature oil field, 3) selected a candidate well for single well pilot test, and 4) successfully completed the pilot test consisting of near miscible CO<sub>2</sub> injection test with two single well chemical tracer tests to determine the effectiveness of CO<sub>2</sub> displacement at near miscible condition.

### **Technology Transfer Events**

The presentations related to this project are summarized as follows:

1. “Improved Predictions of Porosity from Microresistivity Logs in a Mature Field through Incorporation of Pore Typing,” presented at SPE Eastern Regional Meeting, Columbus, Ohio, August 17-19, 2011
2. “Characterization of Potential Sites for Near Miscible CO<sub>2</sub> Application to Improve Oil Recovery in Arbuckle Reservoirs,” presented at RPSEA Onshore Production Conference: Technological Keys to Unlocking Additional Reserves, Lawrence, Kansas, November 8, 2011
3. “Characterization of Potential Sites for Near Miscible CO<sub>2</sub> Application to Improve Oil Recovery in Arbuckle Reservoirs,” presented at RPSEA Onshore Production Conference: Technological Keys to Unlocking Additional Reserves, Golden, Colorado, November 30, 2011
4. “Improved Reservoir Characterization using Petrophysical Classifiers within Electrofacies” presented at SPE IOR Symposium, Tulsa, Oklahoma, April 14-18, 2012
5. “Characterization of Potential Sites for Near Miscible CO<sub>2</sub> Application to Improve Oil Recovery in Arbuckle Reservoirs,” presented at RPSEA Onshore Production Conference: Technological Keys to Unlocking Additional Reserves, Houston, Texas, November 8-9, 2012
6. “Characterization of Potential Sites for Near Miscible CO<sub>2</sub> Application to Improve Oil Recovery in Arbuckle Reservoirs,” presented at Midland CO<sub>2</sub> Conference, Midland, Texas, December 6, 2012

7. "Characterization of Potential Sites for Near Miscible CO<sub>2</sub> Application to Improve Oil Recovery in Arbuckle Reservoirs," presented at RPSEA Onshore Production Conference: Technological Keys to Unlocking Additional Reserves, Wichita, Kansas, June 27, 2013
8. "Improved Oil Recovery with Near Miscible CO<sub>2</sub> Application in Arbuckle Reservoir at Ogallah Field," presented at AAPG Mid-Continent Section Meeting, Wichita, Kansas, October 14, 2013
9. "Single Well Pilot Test of Near Miscible CO<sub>2</sub> Injection in a Kansas Arbuckle Reservoir" presented at SPE IOR Symposium, Tulsa, Oklahoma, April 12-16, 2014

#### Publications and Reports

The publications related to this project are summarized as follows:

1. Teh, W.O., Willhite, G.P., Doveton, J.H., and Tsau, J.S. 2011. Improved Predictions of Porosity from Microresistivity Logs in a Mature field Through Incorporation of Pore Typing. Paper SPE 149506-MS presented at the SPE Eastern Regional Meeting, Columbus, Ohio. August 17-19.
2. Tsau, J.S. 2014. Near Miscible CO<sub>2</sub> Application to Improve Oil Recovery for Small Producers, Phase 2. *TORP Newsletter-Spring*, Lawrence, Kansas.
3. Tsau, J.S., and Ballard, M. 2014. Single Well Pilot Test of Near Miscible CO<sub>2</sub> Injection in a Kansas Arbuckle Reservoir. Paper SPE 169084-MS presented at the SPE Improved Oil Recovery Symposium, Tulsa, Oklahoma, USA. April 12-16.

## ACKNOWLEDGEMENT

The authors wish to acknowledge: Woan Jing Teh for her thesis work in improved reservoir characterization and her geological model later being used in the CO<sub>2</sub> reservoir simulation study; Downing Nelson (Al Downing and Ron Nelson) for providing the tested well for the single well pilot test; Chemical Tracers, Inc. for performing the chemical tracer tests; Praxair for their work in getting the CO<sub>2</sub> downhole at the correct temperature and pressure; Kansas Acid and Weld-Tech for their equipment and personnel availability and their professionalism; G. Paul Willhite, and Jenn-Tai Liang for their useful discussions and input; and Computer Modelling Group (CMG) for making their simulators available and providing fast and friendly tech support. We could not have completed the project without these valuable participants. We also appreciate Martha Cather, the project manager and Charlotte Schroeder, the program manager for their active interest and encouragement throughout this project. Finally, we thank RPSEA and TORP for the support that made this work possible.

Funding for this project is provided by RPSEA through the “Ultra-Deepwater and Unconventional Natural Gas and Other Petroleum Resources” program authorized by the U.S. Energy Policy Act of 2005. RPSEA ([www.rpsea.org](http://www.rpsea.org)) is a nonprofit corporation whose mission is to provide a stewardship role in ensuring the focused research, development and deployment of safe and environmentally responsible technology that can effectively deliver hydrocarbons from domestic resources to the citizens of the United States. RPSEA, operating as a consortium of premier U.S. energy research universities, industry, and independent research organizations, manages the program under a contract with the U.S. Department of Energy’s National Energy Technology Laboratory.

## REFERENCES

Amaefule, J.O., Altunbay, M., Tiab, D., Kersey, D.G. & Keelan, D.K. 1993. Enhanced Reservoir Description: Using Core and Log Data to Identify Hydraulic (Flow) Units and Predict Permeability in Uncored Intervals/Wells. Paper SPE 26436-MS presented at the SPE Annual Technical Conference and Exhibition, October 3, 1993.

Bui, L.H., Tsau, J.S., and Willhite, G. P. 2010. Laboratory Investigations of CO<sub>2</sub> Near Miscible Application in Arbuckle Reservoir. Paper SPE-129710 presented at 2010 SPE Improved Oil Recovery Symposium, Tulsa, April 24-28.

Corey, A. T. 1954. The Interrelations Between Gas and Oil Relative Permeabilities. *Producers Monthly*, November, Vol. 19, p 38-41.

Deans, H.A. and Carlisle, C. T. 1986. Single-Well Tracer Test in Complex Pore Systems. Paper SPE 14886 presented at the SPE/DOE Fifth Symposium on Enhanced Oil Recovery, Tulsa, OK. April 20-23.

Deans, H.A. and Carlisle, C.T. 2007. The Single-Well Chemical Tracer Test – A Method For Measuring Reservoir Fluid Saturations In Situ. *Petroleum Engineering Handbook*, Vol V, Ch. 5, p.615-649.

Focke, J. and Munn, D. 1987. Cementation exponents in Middle Eastern carbonate reservoirs. *SPEFE*, 2 (2): 155-167.

Frailley, S.M., Damico, J. and Leetaru, H.E. 2011. Reservoir Characterization of the Mt. Simon Sandstone, Illinois Basin, USA. *Energy Procedia* 4 5487-5494.

Franseen, E. K., Byrnes, A. P., Cansel, J.R., Steinhauff, D. M., and Carr, T. R. 2004. The Geology of Kansas ARBUCKLE GROUP. *Current Research in Earth Sciences*, Bulletin 250, part 2.

Franseen, E. K., Byrnes, A. P., Cansel, J.R., Steinhauff, D. M., and Carr, T. R., and Dubois, M.K. 2003. Geologic Controls on Variable Character of Arbuckle Reservoirs in Kansas-An Emerging Picture. Kansas Geological Survey, Open-file Report 2003-59

Lucia, F. J. 1983. Petrophysical parameters estimated from visual descriptions of carbonate rocks: a field classification of carbonate pore space. *JPT* 35 (3): 629-637.

Lucia, F. J. 2007. Carbonate Reservoir Characterization: An Integrated Approach. Berlin ; New York: Springer.

Teh, W.O., Willhite, G.P., Doveton, J.H., and Tsau, J.S. 2011. Improved Predictions of Porosity from Microresistivity Logs in a Mature field Through Incorporation of Pore Typing. Paper SPE 149506-MS presented at the SPE Eastern Regional Meeting, Columbus, Ohio. August 17-19.

Teh, W.O., Willhite, G.P., and Doveton, J.H. 2012. Improved Reservoir Characterization using Petrophysical Classifiers within Electrofacies. Paper SPE-154341-PP presented at the SPE Improved Oil Recovery Symposium, Tulsa, Oklahoma, USA. April 14-18.

Teh, W.O. 2012. Improved Reservoir Characterization and Simulation of a Mature Field Using an Integrated Approach. Master thesis, University of Kansas, June.

Tsau, J.S., Bui, L.H., and Willhite, G.P. 2010. Swelling/Extraction Test of a Small Sample Size for Phase Behavior Study. Paper SPE 129728 presented at the Improved Oil Recovery Symposium, Tulsa, OK. April 24-28.

Tsau, J.S. 2010. Near Miscible CO<sub>2</sub> Application to Improve Oil Recovery for Small Producer. RPSEA Final Report 07-123-03.Final, October 29.

Tsau, J.S., and Ballard, M. 2014. Single Well Pilot Test of Near Miscible CO<sub>2</sub> Injection in a Kansas Arbuckle Reservoir. Paper SPE 169084-MS presented at the SPE Improved Oil Recovery Symposium, Tulsa, Oklahoma, USA. April 12-16.